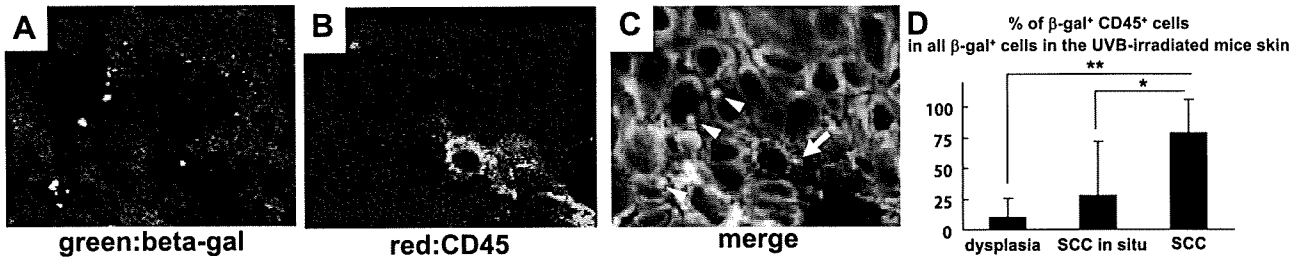

Figure 3. BM-derived infiltrating cells in the UVB-irradiated skin. Triple staining of β-Gal (green) (**A**), CD45 (red) (**B**), and pancytokeratin (cyan) was performed. **C:** Merged image showed β-Gal$^+$/CD45$^+$ (**arrow**) or β-Gal$^+$/CD45$^-$ (**arrowheads**) cells in the tumor. **D:** Percentage of CD45$^+$ of all β-Gal$^+$ cells in the UVB-irradiated mice skin. In all β-Gal$^+$ cells, 10.1 ± 15.3% was positive for CD45 in the epidermal dysplasia lesions, 27.3 ± 44.1% in the SCC *in situ* lesions, and at 78.7 ± 27.4% in the SCC lesions ($^*P < 0.05$, $^{**}P < 0.01$). Original magnifications, ×600.

positive cells in the SCC *in situ* lesions was decreased to 0.25% (Figure 2B). The number of β-Gal-positive cells and total epidermal cells of the UVB-irradiated skin were as follow; unaffected (6 of 2276), dysplasia (28 of 4804), SCC *in situ* (15 of 5445). We further confirmed that no X-Gal-positive cells were detected in untreated (unirradiated) mice. We failed to find any clusters of X-Gal-positive cells in either the unaffected epidermis or the tumor. These results indicate that BMDCs in the UVB-irradiated skin do not commonly give rise to a monoclonal expansion.

After 10 months of UVB irradiation, in the epidermal dysplasia lesions and SCC *in situ* lesions, we found X-Gal-positive cells in a similar location as mice skin that received 5 months of UVB irradiation. In the SCC lesions, X-Gal-positive cells were found within the inner part of the tumor (Figure 2A). X-Gal-positive cells were found at a percentage of 0.59% in the epidermal dysplasia lesions and 0.15% in the SCC *in situ* lesions. These percentages of X-Gal-positive cells in 10-month UVB-irradiated mouse skin were similar to the percentage in 5-month UVB-irradiated mouse skin. In the SCC lesions, the percentage of X-Gal-positive cells was at 0.03%, which decreased in comparison with the percentage in the SCC *in situ* lesions (Figure 2C). The number of β-Gal-positive cells and total epidermal cells of the UVB-irradiated skin were as follow; dysplasia (28 of 5141), SCC *in situ* (9 of 6559), SCC (4 of 13,701).

As an additional test for BM origin, we used a mouse model in which BMDCs were GFP$^+$ using BMT from GFP transgenic mice. Although we evaluated the percentages of BMDCs in UVB-irradiated skin, the GFP$^+$/pancytokeratin$^+$ cells were found at an extremely low percentage, ~0.12% in the epidermal dysplasia lesions and 0% in the SCC *in situ* lesions (data not shown). Previous reports about the *H. felis* gastric cancer also showed a similar tendency that the percentages of malignant cells with the marker of BMDCs was much lower in GFP-labeled model mice than in β-Gal-labeled model mice.[15] Therefore we used an UVB-irradiated mouse model with labeled BMDCs with β-Gal in the following experiments.

Most BMDCs in the SCC Are Inflammatory Hematopoietic Cells

We considered that some X-Gal-positive cells in the UVB-irradiated skin were likely to be the tumor-infiltrating hematopoietic cells. To investigate the presence of these cells, triple staining for β-Gal, CD45 (hematopoietic marker), and a pancytokeratin (cytokeratin marker) was performed (Figure 3, A–C). The number of β-Gal$^+$/CD45$^+$ of all β-Gal$^+$ cells per field was counted in UVB-irradiated mouse skin. In all β-Gal$^+$ cells, 10.1% were positive for CD45 in the epidermal dysplasia lesions. Percentages of CD45$^+$ cells of all β-Gal$^+$ cells were 27.3% and 78.7% in the SCC *in situ* lesions and in the SCC lesions, respectively (Figure 3D). Some of the CD45$^+$ cells were fused with carcinoma cells. Indeed, CD45 has been found to be expressed by cancer cells.[30–32] However, we were unable to find X-Gal-positive cells that co-expressed CD45 and pancytokeratin. The result of our experiments clearly shows that some β-Gal$^+$ cells are tumor-infiltrating hematopoietic cells, whereas other β-Gal$^+$/CD45$^-$ cells might be BMDCs that differentiated into tumor keratinocytes. However, the percentage of β-Gal$^+$/CD45$^+$ cells (indicating tumor-infiltrating hematopoietic cells) is increased in the SCC lesions. This observation would indicate that the actual occurrence rate of BM-derived keratinocytes is lower than our counting of BMDCs that were detected with X-Gal staining.

Small Number of BMDCs in the SCC Exhibited Donor XY Chromosomes

To further confirm BM origin, we analyzed UVB-induced skin SCC cells from female hosts (XX chromosomes) transplanted with male donor BM (XY chromosomes) using fluorescence *in situ* hybridization technique. We counted more than 10,000 cells and detected some donor-derived keratinocytes with XY chromosome expression, indicating BM origin (less than 0.05%) (Figure 4A).

In various organs, BMDCs contribute to the tissue reconstitution by either fusion[22] or transdifferentiation.[19] To determine whether BMDC engraftment into the specific tissue cells was because of differentiation or somatic cell fusion, fluorescence *in situ* hybridization was used because the fused cells would be expected to possess XXXY chromosomes. Although we observed keratinocytes with Y chromosomes in the tumor, none of them expressed an XXXY chromosome. However, fusion hybrids notoriously lose chromosomes and the absence of tetraploid cells does not rule out fusion.[33–35] Therefore, we could not exclude the possibility of cell fusion with the present data.

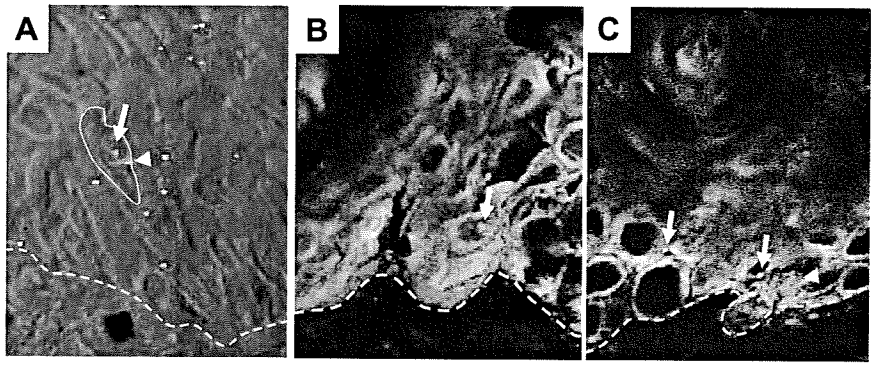

Figure 4. XY chromosome expressions and epidermal stem cell markers of the BMDCs in the UVB-irradiated skin. **A:** Fluorescence *in situ* hybridization showed cells with single X chromosome (red, **arrow**) and single Y chromosome (cyan, **arrowhead**) in the UVB-induced skin SCC. XY chromosome cells, indicating BMDCs were indicated. **B:** Triple staining of β-Gal (green), α6 integrin (red), and pancytokeratin (cyan) was performed. **Arrow** shows β-Gal$^+$ tumor keratinocytes. Although α6 integrin was positive within the edge of the tumor, we could not find any significant overexpression of α6 integrin of β-Gal$^+$/cytokeratin$^+$ cells. **C:** Triple staining of β-Gal (green), BrdU (red), pancytokeratin (cyan). **Arrows** show β-Gal$^+$ tumor keratinocytes. **Arrowhead** shows a BrdU$^+$ tumor keratinocyte. We found no β-Gal$^+$/BrdU$^+$ tumor keratinocytes.

BMDCs in the SCC Failed to Express Epidermal Stem Cell Marker

Although the CSC markers of skin SCC have yet to be defined, published studies suggest that tumor-initiating cells might be positive for the stem cell marker of the original organs.[6,8] To investigate the possibility that BMDCs in the UVB-irradiated skin could share some characteristics of CSCs of skin SCC, we assayed the location of these presumptive CSCs that are positive for epidermal stem cell markers in the UVB-induced skin SCC.

Although CD34 is an established marker of skin epithelial stem cells,[36] none of the keratinocytes (including BM-derived keratinocytes) in the UVB-induced skin SCC expressed CD34 (data not shown). Furthermore, skin epithelial stem cells express elevated levels of α6 integrin compared with differentiated keratinocytes.[37] Although some keratinocytes in the edge of SCC showed α6 integrin expression, β-Gal$^+$/pancytokeratin$^+$ cells (indicating BM-derived keratinocytes) did not show significantly upregulated α6 integrin expression compared with non-BM-derived keratinocytes (Figure 4B). In addition, tissue stem cells can be distinguished from transit-amplifying cells by their ability to incorporate and retain 5-bromo-2′-deoxyuridine (BrdU) throughout a long period of time. Therefore, tissue stem cells can be identified as label-retaining cells (LRCs).[29] To determine whether BMDCs in the UVB-irradiated mouse skin exhibit any LRC characteristics, the tumor-bearing mice were fed water containing BrdU. In the UVB-irradiated mice skin, no LRCs expressed β-Gal (Figure 4C). These results indicate that BMDCs in the UVB-induced skin SCC did not share any of these characters of the presumptive CSCs of the skin SCC.

Discussion

Based on recent investigations that suggest the possibility for BMDCs to be the origin of cancers,[15,38] we used a labeled BMDC mouse model and investigated the role of BMDCs during UVB-induced carcinogenesis. With intermittent UVB irradiation, the epidermal morphology in mouse skin changed from the normal state through dysplasia, SCC *in situ*, and finally to SCC. These histological changes are analogous to the natural phenomenon observed in UVB-induced human skin carcinogenesis. We certainly found BMDCs in UVB-irradiated mouse skin. Our data further suggests that BMDCs are recruited to the UVB-damaged skin and transdifferentiate into epidermal keratinocytes to reconstitute the skin, as we previously reported in wound repair.[20] We show the accelerated recruitment of BMDCs in the epidermal dysplasia lesions and the decreased rate of BMDCs in the SCC lesions. We propose this is attributable to the propagation of non-BM-derived malignant keratinocytes. Although BMDCs are recruited to the UVB-damaged skin and transdifferentiate into unaffected epidermal keratinocytes, BMDCs do not convert into malignant keratinocytes so that the rate of BMDCs relatively decreases as non-BM-derived tumor keratinocytes propagate to form skin SCC.

As a result, we found very few instances of BM-derived keratinocytes in the UVB-irradiated mouse skin. This observation strongly suggests that BMDCs are unlikely to be the origin of UVB-induced skin SCC. The objection will no doubt be raised that BMDCs might lose the expression of BM markers during the continuous UVB irradiation. Therefore we were careful to examine BM-derived keratinocytes in skin SCC with three different BMDC markers (β-Gal, GFP, Y chromosome analysis). Our conclusion is exactly the opposite of the *H. felis*-induced murine gastric carcinoma study.[15] It is reasonable to suppose that the difference in the results between *H. felis*-induced gastric carcinoma study and our UVB-induced skin carcinoma study is partially attributable to the process of carcinogenesis including the type of genetic damage and degree of inflammation. In *H. felis*-induced gastric carcinoma, the pathogenic factor, namely CagA, increases the proliferation of host cells or inhibits cell apoptosis, stimulating the malignant transformation of host cells.[39,40] These processes would be important for cancer progression from BMDCs. In humans, previous reports showed that solid cancers contain BM-derived cancer cells at a low level of 0 to 6% except for lung carcinoma that contains ~20% of BM-derived cancer cells.[23,24] These data further showed that BMDCs do not contribute to skin cancers.[23] Our results are consistent with these observations.

The epidermis is continuously supplied with keratinocytes from the hair follicle bulge stem cells throughout adult life.[41] Most epidermal keratinocytes that acquire

oncogenic mutations are lost during differentiation. Therefore, only long-term resident cells, such as stem cells, have the capacity to accumulate the required number of genetic hits necessary for tumor development. For this reason, it is not unreasonable to assume that these epidermal stem cells in the bulge could acquire oncogenic mutations, transdifferentiate into CSCs, and proliferate as malignant cells in the skin cancer. Although a previous report showed that BMDCs were more frequently found in the bulge area,[42] we could not find such a tendency in our experiments in UVB-induced carcinogenesis. Our previous research in the damaged skin also showed no tendency of BMDC accumulation at specific skin sites.[20] Furthermore, we failed to find any evidence of BMDC clonal expansion in the UVB-irradiated mice skin. We also showed that BMDCs express no epidermal stem cell markers and fail to behave as LRCs, one of the main characteristics of tissue stem cells. Although the existence of the CSCs in the skin cancer has yet to be properly defined, we suggest that the CSCs in the UVB-induced skin SCC, if present, do not commonly originate from BMDCs.

It is important to determine the origin of the CSCs for the elucidation of carcinogenic mechanisms or for the treatment of cancer. Because of the recent reports that showed sarcoma derived from mesenchymal stem cells,[43,44] an objection against transferring cells with the potential to have properties of stem or progenitor cells has arisen in regenerative medicine. However we can conclude from the results of our experiments that cancer cells in the UVB-induced skin SCC do not originate from BMDCs. Therefore we consider that in adopting or using BMDCs for regenerative medicine, the possibility of unexpected carcinogenesis can primarily be excluded and that BMDCs should be further tested and adapted for use in regenerative medicine, especially for skin.

We demonstrated the existence of BM-derived keratinocytes in the UVB-irradiated skin. These BM-derived keratinocytes were considered to be the result of transdifferentiation, not fusion. However, the number of BM-derived keratinocytes was extremely few, with no clonal expansion. Furthermore, BM-derived keratinocytes failed to express the epidermal stem cell markers (CD34, high α6 integrin and LRCs). Through our laboratory experiments, the possibility that BMDCs are the origin of UVB-induced skin SCC is extremely low.

References

1. Alonso L, Fuchs E: Stem cells of the skin epithelium. Proc Natl Acad Sci USA 2003, 100:11830–11835
2. Jordan CT, Guzman ML, Noble M: Cancer stem cells. N Engl J Med 2006, 355:1253–1261
3. Al-Hajj M, Clarke MF: Self-renewal and solid tumor stem cells. Oncogene 2004, 23:7274–7282
4. Lapidot T, Sirard C, Vormoor J, Murdoch B, Hoang T, Caceres-Cortes J, Minden M, Paterson B, Caligiuri MA, Dick JE: A cell initiating human acute myeloid leukaemia after transplantation into SCID mice. Nature 1994, 367:645–648
5. Cox CV, Evely RS, Oakhill A, Pamphilon DH, Goulden NJ, Blair A: Characterization of acute lymphoblastic leukemia progenitor cells. Blood 2004, 104:2919–2925
6. Singh SK, Clarke ID, Terasaki M, Bonn VE, Hawkins C, Squire J, Dirks PB: Identification of a cancer stem cell in human brain tumors. Cancer Res 2003, 63:5821–5828
7. Al-Hajj M, Wicha MS, Benito-Hernandez A, Morrison SJ, Clarke MF: From the cover: prospective identification of tumorigenic breast cancer cells. Proc Natl Acad Sci USA 2003, 100:3983–3988
8. Collins AT, Berry PA, Hyde C, Stower MJ, Maitland NJ: Prospective identification of tumorigenic prostate cancer stem cells. Cancer Res 2005, 65:10946–10951
9. Ricci-Vitiani L, Lombardi DG, Pilozzi E, Biffoni M, Todaro M, Peschle C, De Maria R: Identification and expansion of human colon-cancer-initiating cells. Nature 2007, 445:111–115
10. Li C, Heidt DG, Dalerba P, Burant CF, Zhang L, Adsay V, Wicha M, Clarke MF, Simeone DM: Identification of pancreatic cancer stem cells. Cancer Res 2007, 67:1030–1037
11. Passegué E, Wagner EF, Weissman IL: JunB deficiency leads to a myeloproliferative disorder arising from hematopoietic stem cells. Cell 2004, 119:431–443
12. Bonnet D, Dick JE: Human acute myeloid leukemia is organized as a hierarchy that originates from a primitive hematopoietic cell. Nat Med 1997, 3:730–737
13. Jamieson CHM, Ailles LE, Dylla SJ, Muijtjens M, Jones C, Zehnder JL, Gotlib J, Li K, Manz MG, Keating A, Sawyers CL, Weissman IL: Granulocyte-macrophage progenitors as candidate leukemic stem cells in blast-crisis CML. N Engl J Med 2004, 351:657–667
14. Chaligné R, James C, Tonetti C, Besancenot R, Le Couedic JP, Fava F, Mazurier F, Godin I, Maloum K, Larbret F, Lecluse Y, Vainchenker W, Giraudier S: Evidence for MPL W515L/K mutations in hematopoietic stem cells in primitive myelofibrosis. Blood 2007, 110:3735–3743
15. Houghton J, Stoicov C, Nomura S, Rogers AB, Carlson J, Li H, Cai X, Fox JG, Goldenring JR, Wang TC: Gastric cancer originating from bone marrow-derived cells. Science 2004, 306:1568–1571
16. Petersen BE, Bowen WC, Patrene KD, Mars WM, Sullivan AK, Murase N, Boggs SS, Greenberger JS, Goff JP: Bone marrow as a potential source of hepatic oval cells. Science 1999, 284:1168–1170
17. Ferrari G, Cusella G, Angelis D, Coletta M, Paolucci E, Stornaiuolo A, Cossu G, Mavilio F: Muscle regeneration by bone marrow-derived myogenic progenitors. Science 1998, 279:1528–1530
18. Brazelton TR, Rossi FMV, Keshet GI, Blau HM: From marrow to brain: expression of neuronal phenotypes in adult mice. Science 2000, 290:1775–1779
19. Harris RG, Herzog EL, Bruscia EM, Grove JE, Van Arnam JS, Krause DS: Lack of a fusion requirement for development of bone marrow-derived epithelia. Science 2004, 305:90–93
20. Inokuma D, Abe R, Fujita Y, Sasaki M, Shibaki A, Nakamura H, McMillan JR, Shimizu T, Shimizu H: CTACK/CCL27 accelerates skin regeneration via accumulation of bone marrow-derived keratinocytes. Stem Cells 2006, 24:2810–2816
21. Sasaki M, Abe R, Fujita Y, Ando S, Inokuma D, Shimizu H: Mesenchymal stem cells are recruited into wounded skin and contribute to wound repair by transdifferentiation into multiple skin cell type. J Immunol 2008, 180:2581–2587
22. Nygren JM, Jovinge S, Breitbach M, Sawen P, Roll W, Hescheler J, Taneera J, Fleischmann BK, Jacobsen SEW: Bone marrow-derived hematopoietic cells generate cardiomyocytes at a low frequency through cell fusion, but not transdifferentiation. Nat Med 2004, 10:494–501
23. Cogle CR, Theise ND, Fu D, Ucar D, Lee S, Guthrie SM, Lonergan J, Rybka W, Krause DS, Scott EW: Bone marrow contributes to epithelial cancers in mice and humans as developmental mimicry. Stem Cells 2007, 25:1881–1887
24. Avital I, Moreira AL, Klimstra DS, Leversha M, Papadopoulos EB, Brennan M, Downey RJ: Donor-derived human bone marrow cells contribute to solid organ cancers developing after bone marrow transplantation. Stem Cells 2007, 25:2903–2909
25. Gloster JHM, Neal K: Skin cancer in skin of color. J Am Acad Dermatol 2006, 55:741–760
26. Brash DE, Rudolph JA, Simon JA, Lin A, McKenna GJ, Baden HP, Halperin AJ, Ponten J: A role for sunlight in skin cancer: UV-induced p53 mutations in squamous cell carcinoma. Proc Natl Acad Sci USA 1991, 88:10124–10128
27. Katiyar SK, Korman NJ, Mukhtar H, Agarwal R: Protective effects of

silymarin against photocarcinogenesis in a mouse skin model. J Natl Cancer Inst 1997, 89:556–566
28. Allen SM, Florell SR, Hanks AN, Alexander A, Diedrich MJ, Altieri DC, Grossman D: Survivin expression in mouse skin prevents papilloma regression and promotes chemical-induced tumor progression. Cancer Res 2003, 63:567–572
29. Zhang J, Niu C, Ye L, Huang H, He X, Tong W-G, Ross J, Haug J, Johnson T, Feng JQ, Harris S, Wiedemann LM, Mishina Y, Li L: Identification of the haematopoietic stem cell niche and control of the niche size. Nature 2003, 425:836–841
30. Ngo N, Patel K, Isaacson PG, Naresh KN: Leucocyte common antigen (CD45) and CD5 positivity in an "undifferentiated" carcinoma: a potential diagnostic pitfall. J Clin Pathol 2007, 60:936–938
31. Collette M, Descamps G, Pellat-Deceunynck C, Bataille R, Amiot M: Crucial role of phosphatase CD45 in determining signaling and proliferation of human myeloma cells. Eur Cytokine Netw 2007, 18:120–126
32. Huysentruyt LC, Mukherjee P, Banerjee D, Shelton LM, Seyfried TN: Metastatic cancer cells with macrophage properties: evidence from a new murine tumor model. Int J Cancer 2008, 123:73–84
33. Pawelek JM, Chakraborty AK: Fusion of tumour cells with bone marrow-derived cells: a unifying explanation for metastasis. Nat Rev Cancer 2008, 8:377–386
34. Yilmaz Y, Lazova R, Qumsiyeh M, Cooper D, Pawelek J: Donor Y chromosome in renal carcinoma cells of a female BMT recipient: visualization of putative BMT-tumor hybrids by FISH. Bone Marrow Transplant 2005, 35:1021–1024
35. Chakraborty A, Lazova R, Davies S, Backvall H, Ponten F, Brash D, Pawelek J: Donor DNA in a renal cell carcinoma metastasis from a bone marrow transplant recipient. Bone Marrow Transplant 2004, 34:183–186
36. Tumbar T, Guasch G, Greco V, Blanpain C, Lowry WE, Rendl M, Fuchs E: Defining the epithelial stem cell niche in skin. Science 2004, 303:359–363
37. Tani H, Morris RJ, Kaur P: Enrichment for murine keratinocyte stem cells based on cell surface phenotype. Proc Natl Acad Sci USA 2000, 97:10960–10965
38. Simka M: Do nonmelanoma skin cancers develop from extra-cutaneous stem cells? Int J Cancer 2008, 122:2173–2177
39. Saadat I, Higashi H, Obuse C, Umeda M, Murata-Kamiya N, Saito Y, Lu H, Ohnishi N, Azuma T, Suzuki A, Ohno S, Hatakeyama M: Helicobacter pylori CagA targets PAR1/MARK kinase to disrupt epithelial cell polarity. Nature 2007, 447:330–333
40. Smith MG, Hold GL, Tahara E, El-Omar EM: Cellular and molecular aspects of gastric cancer. World J Gastroenterol 2006, 12: 2979–2990
41. Lavker RM, Sun T-T: Epidermal stem cells: properties, markers, and location. Proc Natl Acad Sci USA 2000, 97:13473–13475
42. Brittan M, Braun KM, Reynolds LE, Conti FJ, Reynolds AR, Poulsom R, Alison MR, Wright NA, Hodivala-Dilke KM: Bone marrow cells engraft within the epidermis and proliferate in vivo with no evidence of cell fusion. J Pathol 2005, 205:1–13
43. Tirode F, Laud-Duval K, Prieur A, Delorme B, Charbord P, Delattre O: Mesenchymal stem cell features of Ewing tumors. Cancer Cell 2007, 11:421–429
44. Aguilar S, Nye E, Chan J, Loebinger M, Spencer-Dene B, Fisk N, Stamp G, Bonnet D, Janes SM: Murine but not human mesenchymal stem cells generate osteosarcoma-like lesions in the lung. Stem Cells 2007, 25:1586–1594

LETTER

Secondary syphilis mimicking warts in an HIV-positive patient

A 35-year-old Japanese man visited our hospital with a 2-year history of skin lesions affecting his palms and soles. The palmar lesions comprised diffuse papillomatous hyperkeratotic and macerative reddish skin eruptions (fig 1A). In addition, he had warty-like plaques of 4.5 cm in diameter on his right sole (fig 1B). Upon his initial visit, he did not report any other symptoms such as chills or malaise. These unusual and severe hyperkeratotic lesions did not fit any typical known skin disease such as verruca, Reiter's syndrome and so on.

Skin biopsy specimens of the hyperkeratotic lesions on the palm and sole showed marked exophytic papillomatous acanthosis with a few koilocytotic cells. In the upper dermis, a dense inflammatory infiltrate containing large numbers of plasma cells was present.

Clinical and histopathological findings led us to suspect syphilis. The serological test showed high reactivity of the rapid plasma reagin test for syphilis at a titre of 1 : 1024 and a positive *Treponema pallidum* haemagglutination test (2450TU). Around the same time, numerous spirochaetes were detected from his swollen tonsils with Indian ink staining of the smear.

In addition, we suspected that he was in an immunodeficient state because of his severe clinical features of syphilis, therefore we performed a supplementary study. In the following results, a viral serological test revealed that he had detectable antibodies to HIV-1 (HIV viral load 11 000 copies/ml). The CD4 cell count (479 cells/mm^3) was slightly decreased.

After 3 weeks of penicillin antibiotic treatment, his skin eruptions and swollen tonsils had dramatically improved (fig 1C, D). Furthermore, we could not detect any evidence suggesting human papillomavirus infection using a method that can detect a broad range of DNA from multiple human papillomavirus types in both the palm and sole lesions.[1] Finally, we diagnosed his hyperkeratotic skin lesions and enlarged tonsils as secondary syphilis because of the good response to the antibiotic treatment and pathological and serological findings. Furthermore, we suspected his immunodeficiency from the atypical skin eruptions and reached a diagnosis of HIV infection.

Infections with unusual clinical features are frequently observed in patients with HIV.[2] In recent years, some cases of syphilis in HIV patients with various manifestations and a rapidly progressive course have been reported, which have led to the hypothesis that HIV superinfection modifies the clinical presentation and disease course of syphilis.[2 3]

Secondary syphilis has various clinical forms, such as macular syphilide, papular syphilide, pustular ulcerative syphilide and syphilitic alopecia.[4] In papular syphilide, there are several subtypes including syphilitic psoriasis and condyloma latum, which may present as slightly hyperkeratotic lesions. It has been reported that a very small number of syphilis patients manifest severe palmoplantar keratoderma such as that seen in Reiter's syndrome.[5 6]

As this patient exhibited such significant and atypical clinical features, we were able to diagnose HIV infection. This case emphasises the importance of suspecting and checking for HIV infection after a rare clinical presentation of secondary syphilis, such as these severe wart-like hyperkeratotic lesions.

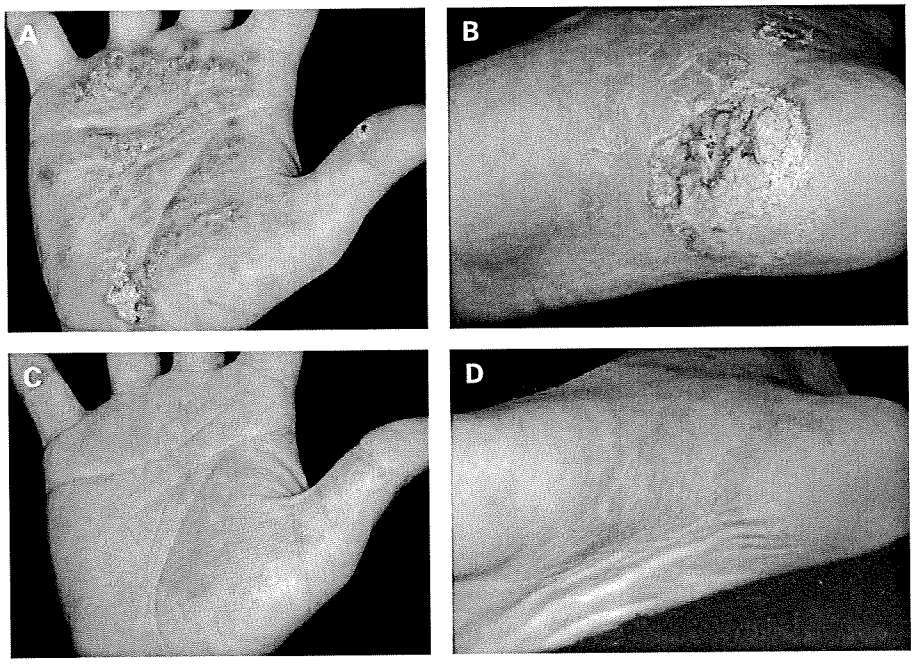

Figure 1 Skin changes on the right palm (A) and sole (B) on the initial visit. After penicillin antibiotic treatment, the skin lesions had completely disappeared (C, D).

S Shinkuma, R Abe, M Nishimura, K Natsuga, Y Fujita, T Nomura, W Nishie, H Shimizu

Department of Dermatology, Hokkaido University Graduate School of Medicine, Sapporo, Japan

Correspondence to: Dr S Shinkuma, Department of Dermatology, Hokkaido University Graduate School of Medicine, N15 W7, Sapporo 060-8638, Japan; qxfjc346@ybb.ne.jp

Competing interests: None.

Ethics approval: Ethics approval was obtained.

Patient consent: Obtained.

Provenance and peer review: Not commissioned; externally peer reviewed.

Accepted 24 February 2009

Sex Transm Infect 2009;**85**:484.
doi:10.1136/sti.2008.035626

REFERENCES

1. **Forslund O,** Antonsson A, Nordin P, *et al*. A broad range of human papillomavirus types detected with a general PCR method suitable for analysis of cutaneous tumours and normal skin. *J Gen Virol* 1999;**80**:2437–43.
2. **Penneys NS,** Hicks B. Unusual cutaneous lesions associated with acquired immunodeficiency syndrome. *J Am Acad Dermatol* 1985;**13**:845–52.
3. **Gregory N,** Sanchez M, Buchness MR. The spectrum of syphilis in patients with human immunodeficiency virus infection. *J Am Acad Dermatol* 1990;**22**:1061–7.
4. **Morton RS,** Kinghorn GR, Kerdel-Vegas F. The Treponematoses. In: Burns T, Breathnach S, Cox N, Griffiths C, eds. *Rook's textbook of dermatology*, 7th edn. Oxford: Blackwell Science Ltd, 2004:30.1–30.28.
5. **Kishimoto M,** Lee MJ, Mor A, *et al*. Syphilis mimicking Reiter's syndrome in an HIV-positive patient. *Am J Med Sci* 2006;**332**:90–2.
6. **Radolf JD,** Kaplan RP. Unusual manifestations of secondary syphilis and abnormal humoral immune response to *Treponema pallidum* antigens in a homosexual man with asymptomatic human immunodeficiency virus infection. *J Am Acad Dermatol* 1988;**18**:423–8.

Correspondence

Scleroedema adultorum associated with sarcoidosis

doi: 10.1111/j.1365-2230.2009.03423.x

Sarcoidosis is a systemic granulomatous disease of unknown aetiology that displays a wide variety of skin features including maculopapules, nodules, plaques, subcutaneous nodules, infiltrative scars, and lupus pernio.[1] We report a case of sarcoidosis with subcutaneous induration of the neck.

A 62-year-old Japanese man presented with a 6-month history of asymptomatic, firm indurations on the neck. He had first noticed these skin lesions after bilateral symmetrical hilar lymph-node enlargement was found during routine chest radiography. Transbronchial biopsies resulted in the histological identification of non-caseating granulomas compatible with sarcoidosis. The patient had no history of diabetes mellitus or preceding infection.

On physical examination, symmetrical, hard, nonpitting indurations of the skin were found on the posterior neck (Fig. 1a). The patient's general health was good.

Results of routine laboratory studies including angiotensin-converting enzyme and tuberculin response gave normal results, and there was no evidence of monoclonal proteinaemia. Computed tomography scans showed bilateral hilar lymphadenopathy but there was no other lymphadenopathy noted.

Histological examination of skin-biopsy specimens taken from the posterior neck revealed swelling of the dermal collagen bundles without increase in fibroblast numbers, and the subcutaneous fat had been replaced by collagen fibres (Fig. 1b). A diagnosis of SA was made. Treatment was started with steroid ointment or 9 months, but without evident improvement.

SA is a rare disorder of unknown cause, but often complicates diabetes mellitus. In such cases, the lesions are usually limited to neck and upper back, and tend to be persistent.[2] In contrast, in SA not associated with diabetes mellitus, the lesions often spread to the face, trunk and upper arms, but may spontaneously subside.[3,4] However, in spite of no obvious association with diabetes mellitus, our patient had intractable induration distributed over a localized area. Interestingly, in this case, development of the skin lesion was coincidental with the diagnosis of sarcoidosis. The clinical appearance was indicative of scleroedema. There have been no previous reports of any association between SA and sarcoidosis. Therefore, we first suspected a subcutaneous form of sarcoidosis rather than scleroedema. However, the histopathological findings confirmed a diagnosis of scleroedema.

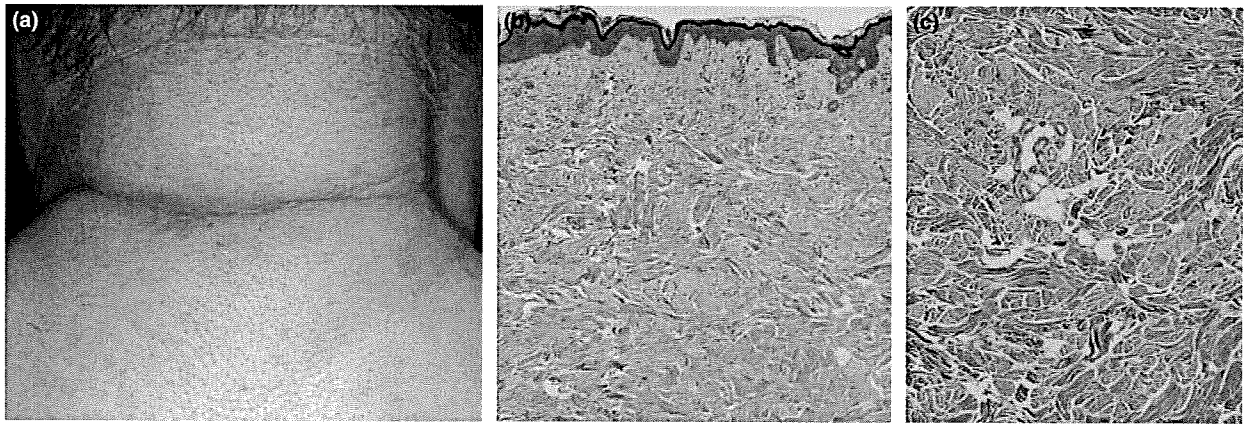

Figure 1 (a) Symmetrical, hard, nonpitting induration on the posterior side of the neck; (b) inflammatory cell infiltration in the upper dermis and swelling of collagen bundles in the lower dermis; (c) swelling of the dermal collagen bundles without any increase in fibroblast numbers, and the replacing of subcutaneous fatty tissues by collagen fibres.

Sarcoidosis is known to be complicated by a variety of immunological diseases including malignant lymphoma, autoimmune diseases and multiple myeloma, and scleroedema is associated with infections, paraproteinaemia and multiple myeloma. Some previous studies have shown an increase in amounts of proα1(I) collagen mRNA in both sarcoidosis and scleroedema lesions.[5] Some common factors in the pathogenesis of two diseases might therefore be involved in this patient.

D. Inokuma, D. Sawamura,* A. Shibaki, R. Abe and H. Shimizu

*Department of Dermatology, Hokkaido University Graduate School of Medicine, North 15 West 7, Kita-ku, Sapporo, 060-8638, Japan; and *Department of Dermatology, Hirosaki University Graduate School of Medicine, Hirosaki CIty, Japan*

E-mail: inokuma@med hokudai.ac.jp

Conflict of interest: none declared.

Accepted for publication 7 January 2009

References

1 Young RJ III, Gilson RT, Yanase D *et al.* Cutaneous sarcoidosis. *Int J Dermatol* 2001; **40**: 249–53.

2 Farrell AM, Branfoot AC, Moss J *et al.* Scleredema diabeticorum of Buschke confined to the thighs. *Br J Dermatol* 1996; **134**: 1113–15.

3 Basarab T, Burrows NP, Munn SE *et al.* Systemic involvement in scleredema of Buschke associated with IgG-kappa paraproteinaemia. *Br J Dermatol* 1997; **136**: 939–42.

4 Ratip S, Akin H, Ozdemirli M *et al.* Scleredema of Buschke associated with Waldenstrom's macroglobulinaemia. *Br J Dermatol* 2000; **143**: 450–2.

5 Tasanen PO. Demonstration of increased levels of type I collagen mRNA using quantitative polymerase chain reaction in fibrotic and granulomatous skin diseases. *Br J Dermatol* 1998; **139**: 23–6.

Carcinogenesis vol.30 no.9 pp.1597–1605, 2009
doi:10.1093/carcin/bgp160
Advance Access publication July 7, 2009

Deficient deletion of apoptotic cells by macrophage migration inhibitory factor (MIF) overexpression accelerates photocarcinogenesis

Ayumi Honda[1,2,†], Riichiro Abe[2,†], Yoko Yoshihisa[1], Teruhiko Makino[1], Kenji Matsunaga[1], Jun Nishihira[3], Hiroshi Shimizu[2] and Tadamichi Shimizu[1,*]

[1]Department of Dermatology, Graduate School of Medicine and Pharmaceutical Sciences, University of Toyama, Sugitani, Toyama 930-0194, Japan, [2]Department of Dermatology, Hokkaido University Graduate School of Medicine, Sapporo 060-8638, Japan and [3]Department of Medical Information, Hokkaido Information University, Ebetsu 069-8585, Japan

*To whom correspondence should be addressed. Tel: +81 76 434 7305; Fax: +81 76 434 5028;
Email: shimizut@med.u-toyama.ac.jp

Chronic ultraviolet (UV) exposure can increase the occurrence of p53 mutations, thus leading to a dysregulation of apoptosis and the initiation of skin cancer. Therefore, it is extremely important that apoptosis is induced quickly after UV irradiation, without any dysregulation. Recent studies have suggested a potentially broader role for macrophage migration inhibitory factor (MIF) in growth regulation via its ability to antagonize p53-mediated gene activation and apoptosis. To further elucidate the possible role of MIF in photocarcinogenesis, the acute and chronic UVB effect in the skin was examined using macrophage migration inhibitory factor transgenic (MIF Tg) and wild-type (WT) mice. The MIF Tg mice exposed to chronic UVB irradiation began to develop skin tumors after ~14 weeks, whereas the WT mice began to develop tumors after 18 weeks. A higher incidence of tumors was observed in the MIF Tg in comparison with the WT mice after chronic UVB irradiation. Next, we clarified whether the acceleration of photo-induced carcinogenesis in the MIF Tg mice was mediated by the inhibition of apoptosis There were fewer sunburned cells in the epidermis of the MIF Tg mice than the WT mice after acute UVB exposure. The epidermis derived from the MIF Tg mice exhibited substantially decreased levels of p53, bax and p21 after UVB exposure in comparison with the WT mice. Collectively, these findings suggest that chronic UVB exposure enhances MIF production, which may inhibit the p53-dependent apoptotic processes and thereby induce photocarcinogenesis in the skin.

Introduction

Exposure to ultraviolet (UV) radiation leads to various acute deleterious cutaneous effects including sunburn and immunosuppression and also long-term consequences such as premature aging and the potential development of skin cancers (1). UV radiation, particularly UVB, which has a wavelength of between 280 and 320 nm, has been suggested epidemiologically and has been demonstrated experimentally to be the pivotal causal factor for skin cancer in humans and other animals (2). Chronic UVB-induced inflammation and directly damaged DNA can be correlated with skin tumor formation (3,4). Furthermore, the inability to adequately repair DNA after UVB irradiation can result in the formation of skin cancers (5). Chronic UV exposure can increase p53 mutations, thus leading to a dysregulation of apoptosis, an expansion of mutated keratinocytes and the initiation of skin cancer (6).

Abbreviations: CPD, cyclobutane pyrimidine dimmer; IL, interleukin; MIF, macrophage migration inhibitory factor; MIF Tg, macrophage migration inhibitory factor transgenic; mRNA, messenger RNA; PBS, phosphate-buffered saline; TUNEL, terminal deoxynucleotidyl transferase nick end labeling; TNF, tumor necrosis factor; UV, ultraviolet; WT, wild-type.

[†]These authors contributed equally to this work.

There is emerging evidence that keratinocytes participate in cutaneous inflammatory reactions and immune responses by producing a variety of cytokines. UV irradiation may trigger cutaneous inflammatory responses by stimulating epidermal keratinocytes to produce biologically potent cytokines such as interleukin (IL)-1 (7,8), IL-6 (9) and tumor necrosis factor (TNF)-α (10). These cytokines are involved not only in the mediation of local inflammatory reactions but also play discrete roles in tumor promotion (11).

The cytokine macrophage migration inhibitory factor (MIF) was first discovered 40 years ago as a T-cell-derived factor that inhibited the random migration of macrophages (12,13). Recently, MIF was reevaluated as a proinflammatory cytokine and pituitary-derived hormone that potentiates endotoxemia (14). Subsequent work has showed that T cells and macrophages secrete MIF in response to glucocorticoids as well as upon activation by various proinflammatory stimuli (15). It has been reported that MIF is expressed primarily in T cells and macrophages; however, recent studies have revealed this protein to be ubiquitously expressed in various cells (16–20). Skin melanoma cells express MIF messenger RNA (mRNA) and produce MIF protein (21). The expression of MIF mRNA and the production of MIF protein have been shown to be much higher in human melanoma cells than in cultured normal melanocytes. Therefore, MIF functions as a novel growth factor that stimulates uncontrolled growth and invasion of tumor cells (16,21,22). In addition, recent studies have suggested a potentially broader role for MIF in growth regulation because of its ability to antagonize p53-mediated gene activation and apoptosis (23,24).

In the skin, keratinocytes are capable of producing a variety of cytokines and are thought to be a principal source of cytokines from the epidermis after UV irradiation. Previous studies have shown enhanced MIF production in the skin after UVB irradiation (25,26). Solar UV light is a combination of both UVB and UVA wavelengths, each of which stimulate MIF production in both keratinocytes and fibroblasts in the skin. To further elucidate the possible role of MIF in UV-induced carcinogenesis and cell apoptosis, the acute and chronic effect of UVB in skin carcinogenesis was examined using macrophage migration inhibitory factor transgenic (MIF Tg) mice.

Materials and methods

Materials

The following materials were obtained from commercial sources. The Isogen RNA extraction kit was obtained from Nippon Gene (Tokyo, Japan); the DNA random primer labeling kit from Takara (Kyoto, Japan); [^{32}P]dCTP from DuPont-NEN (Boston, MA); anti-CPDs polyclonal antibody from Cosmo Bio Co, Ltd (Tokyo, Japan); anti-p53 polyclonal antibody from Novocastra Lab (Newcastle, UK); anti-p21 polyclonal antibody and anti-BAX polyclonal antibody from Santa Cruz Biotechnology (Santa Cruz, CA) and anti-β-actin antibodies purchased from Sigma–Aldrich Co (St Louis, MO); the western blot detection system was obtained from Cell Signaling Technology (Beverly, MA). The anti-MIF polyclonal antibody was prepared as described previously (27). The Cell Death Detection Kit was provided from Roche Molecular Biochemicals (Indianapolis, IN). Other reagents were of analytical grade.

Mice

The MIF-overexpressed transgenic mice were established following cDNA microinjection and the physical and biochemical characteristics, including body weight, blood pressure, serum levels of cholesterol and blood sugar, were normal as reported previously (28). The expression of the transgene was regulated by a hybrid promoter composed of the cytomegalovirus enhancer and β-actin/β-globin promoter, as reported previously (29). Strain of original MIF-Tg is ICR and backcrossed with C57BL/6 for at least 10 generations. Tg mice were maintained by heterozygous sibling mating. Transgenic and wild-type (WT) mice were maintained under specific-pathogen-free conditions at the Institute for Animal Experiments of Hokkaido University School of Medicine. Experiments using mice were conducted according to the guidelines set out by

the Hokkaido University Institutional Animal Care and Use Committee under an approved protocol. All experiments were performed on 8-week-old male adult mice.

UVB irradiation

UVB light source was a FL20SE30 (Clinical Supply Co, Tokyo, Japan) fluorescent lamp that emits 1.0 mW/cm^2 of UV between 280 and 370 nm (peak 305 nm) at a distance of 25 cm, as measured by UV radiometer (Torex Co, Tokyo, Japan). In short-term UVB experiments, MIF Tg and WT mice had their backs shaved with electric clippers and exposed to 200 mJ/cm^2 UVB. After UVB irradiation, the mice were euthanized at the indicated time points. Skin sections were excised from the dorsal surface and used for western blot analyses or immunohistochemical staining. In some experiments for UVB-induced cutaneous inflammation, UVB radiation was administered three times weekly (on days 1, 3 and 5) and skin was obtained on day 7. To examine UVB-induced carcinogenesis, MIF Tg and WT mice had their backs shaved with electric clippers once a week and were UVB irradiated in separate compartments of a modified mouse cage. An incrementally graded UV protocol was used (30): three times weekly a UV dose was delivered of 2.25 kJ/m^2 for 12 treatments (weeks 1–4), 4.05 kJ/m^2 for 24 treatments (weeks 5–12), 5.1 kJ/m^2 for 12 treatments (weeks 13–16) and 6 kJ/m^2 for 33 treatments (week 17 to the end of the experiment at the 27th week).

Skin tumors

Mice were monitored for tumor formation each week. The time to tumor development was taken as the time up to the appearance of a palpable swelling >1 mm subsequently diagnosed as a tumor on histopathological examination after 27 weeks. The tumor size was estimated after 27 weeks using orthogonal linear measurements made with Vernier calipers according to the following formula: volume (mm^3) = [(width, mm)^2 × (length, mm)]/2. The tumors were excised and preserved in 10% formalin, sectioned, stained with hematoxylin and eosin and examined microscopically. The groups each contained 12 MIF Tg and 12 WT mice.

Northern blot analysis

Total cellular RNA was isolated from the epidermis using an Isogen extraction kit according to the manufacturer's protocol. The epidermis was separated from the dermis by incubation in 0.5% dispase in RPMI 1640 at 37°C for 1 h. RNA was quantified by spectrophotometry and equal amounts of RNA (10 μg) from each sample were loaded on a formaldehyde–agarose gel. The gel was stained with ethidium bromide to visualize the RNA standards and the RNA was transferred onto a nylon membrane. Fragments obtained by restriction enzyme treatment for MIF and glyceraldehyde-3-phosphate dehydrogenase were labeled with [α-^{32}P]dCTP using a DNA random primer labeling kit. Hybridization was carried out using the mouse MIF cDNA probe as previously described (28). The membrane was washed twice with 2× saline and sodium citrate (16.7 mM NaCl, 16.7 mM sodium citrate) at 22°C for 5 min, twice with 0.2× saline and sodium citrate containing 0.1% sodium dodecyl sulfate at 65°C for 15 min and twice with 2× saline and sodium citrate at 22°C for 20 min prior to autoradiography. A quantitative densitometric analysis was performed using an MCID Image Analyzer (Fuji Film, Tokyo, Japan). The density of MIF bands was normalized by the intensities of glyceraldehyde-3-phosphate dehydrogenase.

Western blot analysis

The epidermis of each mouse was homogenized with a Polytron homogenizer (Kinematica, Lausanne, Switzerland). The protein concentrations of the cell homogenates were quantified using a Micro BCA protein assay reagent kit. Equal amounts of homogenates were dissolved in a 20 μl solution contained of Tris–HCl, 50 mM (pH 6.8), containing 2-mercaptoethanol (1%), sodium dodecyl sulfate (2%), glycerol (20%) and bromophenol blue (0.04%) and the samples were heated to 100°C for 5 min. The samples were then subjected to sodium dodecyl sulfate–polyacrylamide gel electrophoresis and electrophoretically transferred onto a nitrocellulose membrane. The membranes were blocked with 1% non-fat dry milk powder in phosphate-buffered saline (PBS), probed with antibodies against p53, bax and p21 and subsequently reacted with secondary IgG antibodies coupled with horseradish peroxidase. The resultant complexes were processed for the detection system according to the manufacturer's protocol. The relative amounts of proteins associated with specific antibodies were normalized according to the intensities of β-actin.

Immunohistochemical analysis

Five micrometers thick section of dorsal skin were fixed in 10% neutral buffered formalin. After deparaffinization, the sections were treated with target retrieval solution (DAKO, Carpinteria, CA), washed three times with PBS and incubated in H_2O_2/methanol/PBS solution (1:50:50) for 15 min to block endogenous peroxidase activity. After three washes in PBS with 0.5% Tween, the sections were preincubated for 10 min in 10% normal goat serum in PBS and then were incubated with the first antibody overnight at 4°C. After three washes in PBS plus 0.5% Tween, the sections were incubated for 1 h at room temperature with the secondary antibodies. After washing in PBS, staining was performed using the Vectastain Elite ABC kit with diaminobenzidine as the chromagen, according to the manufacturer's instructions (Vector Laboratories, Burlingame, CA). As a negative control, the tissue sections were stained with normal serum and the secondary antibody.

UVB-induced apoptosis in cultured keratinocytes of MF Tg and WT. Mouse keratinocyte (second passage) from MIF Tg or C57BL/6 mice were irradiated with UVB at 50 mJ/cm^2. After 24 h, irradiated cells were analyzed for terminal deoxynucleotidyl transferase nick end labeling (TUNEL) assay or western blot for p53.

TUNEL assay. Cells undergoing apoptosis were detected using TUNEL according to the manufacturer's recommended procedure (R&D Systems, Minneapolis, MN). For statistical analysis, apoptotic cells were counted by light microscopy (×100) and expressed as the mean number (±SD) of apoptotic cells per section. Five random fields per section (one section per mouse, five mice per group) were analyzed.

Cultured apoptotic cells were also detected using TUNEL. Incorporated fluorescein was detected by anti-fluorescein monoclonal antibody Fab fragments from sheep, conjugated with alkaline phosphatase.

Statistics

Values are expressed as the mean ± SEM of the respective test or control group. Statistical significance between the control group and test groups was evaluated by either the Student's *t*-test or one-way analysis of variance.

Results

Enhanced expression of MIF in MIF Tg mice epidermis

MIF expression in the MIF Tg mouse epidermis was first examined after UVB irradiation. Northern blot analysis revealed that 16 h after 200 mJ/cm^2 UVB irradiation, MIF Tg mice showed higher levels of MIF mRNA expression even before irradiation. After UVB exposure, the MIF mRNA expression dramatically increased in comparison with that of the WT mice (Figure 1).

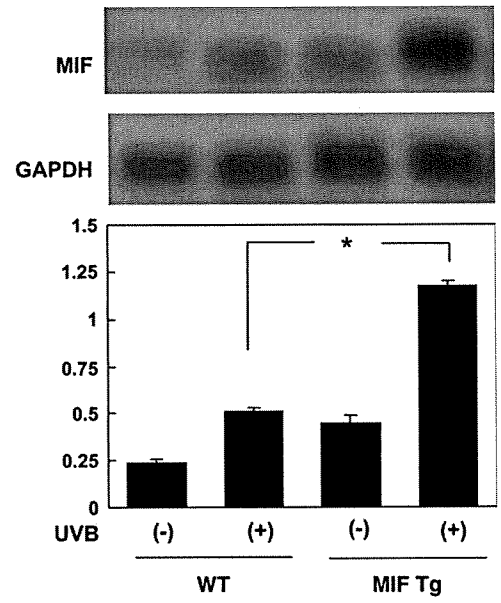

Fig. 1. Enhanced expression of MIF in the MIF Tg mouse epidermis after UV exposure. The expression of MIF mRNA was examined. Total RNA was isolated at 16 h after UVB (200 mJ/cm^2) and analyzed by northern blotting. MIF Tg mice (n = 5) showed higher levels of MIF mRNA expression even before irradiation. After UVB exposure, MIF mRNA expression dramatically increased in comparison with that of WT mice (n = 5). The experiments were repeated three times with similar results.

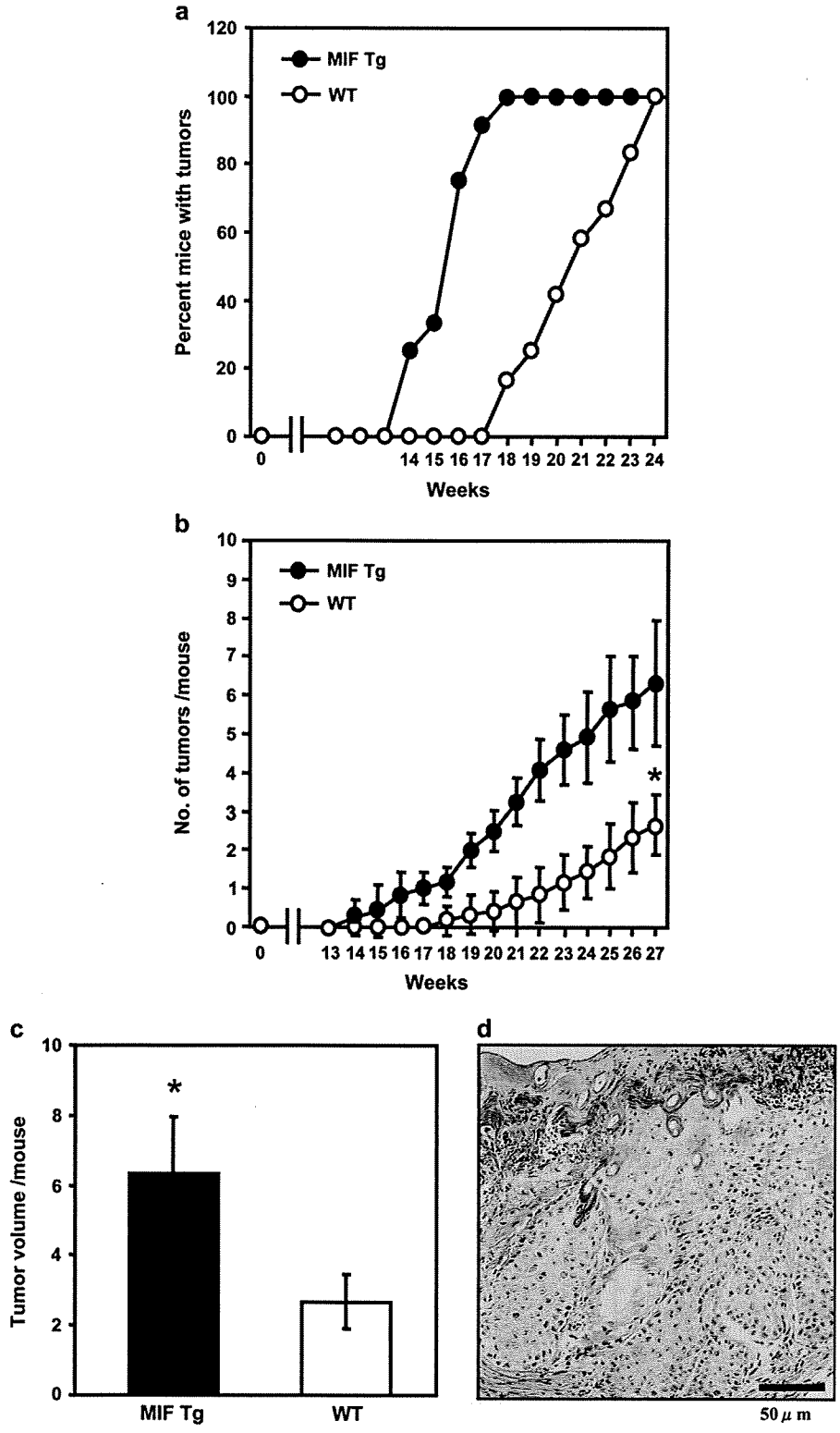

Fig. 2. Accelerated UVB-induced carcinogenesis in the MIF Tg mice. (**a**) MIF Tg and WT mice were subjected to chronic UVB. The details of the protocols are described in Materials and Methods. The formation of skin tumors was determined on a weekly basis. MIF Tg mice exposed to chronic UVB began to develop skin tumors after ~14 weeks, whereas the WT mice began to develop tumors after 18 weeks. (**b**) The incidence of skin tumors was recorded weekly and a tumor was considered to occur when an outgrowth of >1 mm in diameter was observed. MIF Tg mice developed a higher number of tumors in each mouse in comparison with WT mice ($^*P < 0.001$). (**c**) The mice were UVB irradiated as in (b). At the end of study at week 27, the volume of all tumors on each mouse was recorded ($^*P < 0.001$). (**d**) The histopathology of well-differentiated squamous cell carcinoma from an MIF Tg mouse. Scale bar indicates 100 μm (hematoxylin and eosin staining).

Sensitivity of MIF Tg mice to the development of skin tumors elicited by chronic exposure to UVB

To examine the role of MIF for chronic UV-induced carcinogenesis, MIF Tg and WT mice were subjected to chronic UVB as described in the Materials and Methods and followed up for the formation of skin tumors on a weekly basis. The MIF Tg mice exposed to chronic UVB began to develop skin tumors after ~14 weeks, whereas WT mice began to develop tumors after 18 weeks (Figure 2a). The mean time for tumor development in MIF Tg mice was after 110.3 ± 9.0 days, whereas it was 147.0 ± 15.5 days in WT mice. MIF Tg mice developed a higher number of tumors in each mouse in comparison with WT mice. At the 27th week, the average number of tumors per mouse was 6.33 ± 1.61 in the MIF Tg mice, whereas there were only 2.67 ± 0.78 in the WT mice ($P < 0.001$; Figure 2b). The volume of tumors developed in UVB-irradiated MIF Tg mice was significantly higher in comparison with that of WT mice ($P < 0.001$) (Figure 2c). Tumors measuring <2 mm in diameter proved to be too small for a reliable histological analysis and were assumed to be papillomas. Lesions that were ~2 mm in diameter had multilayered epithelia with irregular cells. These lesions were similar to actinic keratosis, and some large tumors (>3 mm in diameter) were diagnosed as well-differentiated SCC (Figure 2d). Twelve unirradiated MIF Tg mice and 12 unirradiated WT mice developed no tumors during the course of this study.

TUNEL-positive cells in UV-irradiated MIF Tg mouse epidermis

The possible role of MIF in UV-induced cell apoptosis was examined using MIF Tg and WT mice. Twenty-four hours after 200 mJ/cm^2 UVB irradiation, large numbers of sunburned cells and TUNEL-positive cells were detected in the WT mice, whereas, there were fewer sunburned cells and TUNEL-positive cells detected in MIF Tg mice (Figure 3a). Thereafter, the number of TUNEL-positive nuclei in the MIF Tg mice was compared with that in the WT mice. MIF Tg mice showed a significantly smaller number of apoptotic cells than the WT mice ($P < 0.01$; Figure 3b).

Immunohistochemistry: accumulation of DNA damages in the epidermis following UVB. We then investigated cyclobutane pyrimidine dimmers (CPD), as UV-induced DNA damage photoproduct

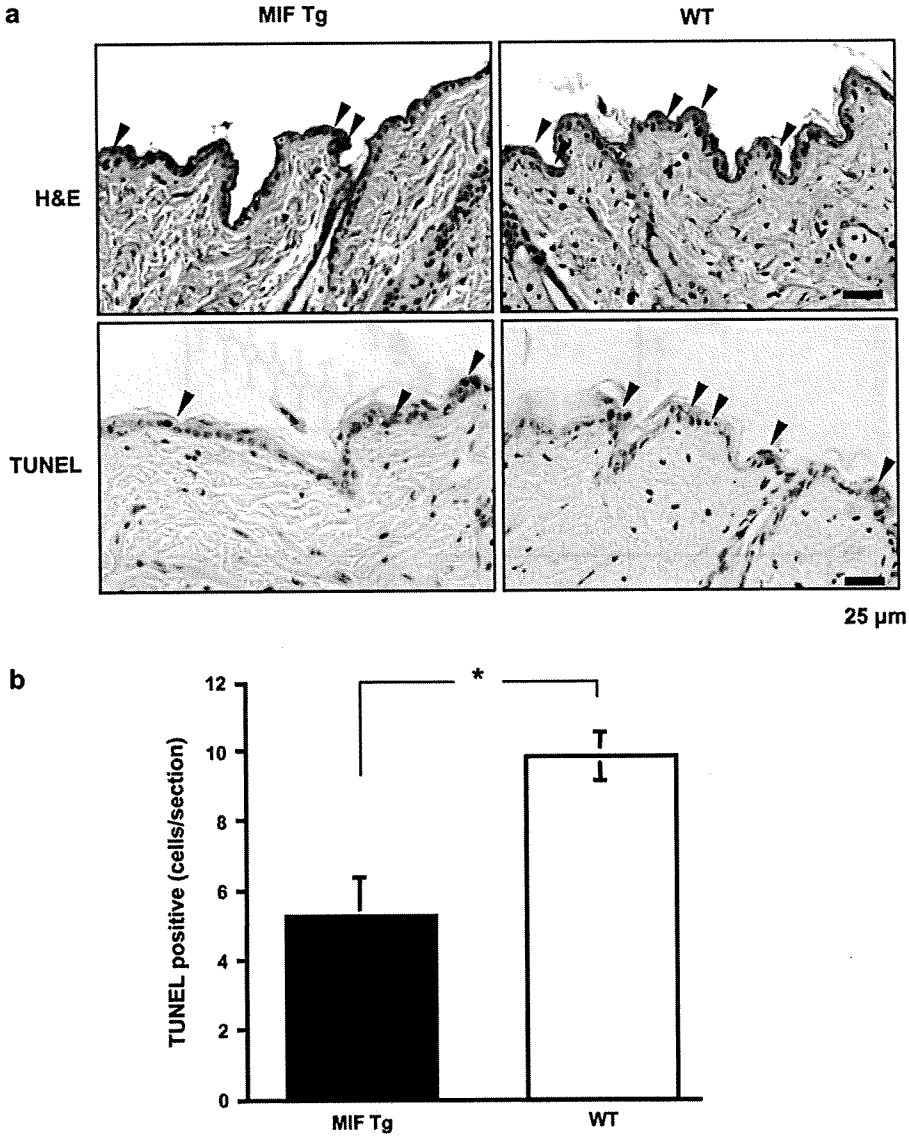

Fig. 3. Sunburn cells in UV-irradiated MIF Tg mouse epidermis. **(a)** Hematoxylin and eosin (H&E) staining and TUNEL assay for the detection of apoptotic cells in the epidermis of MIF Tg and WT mice skin 24 h after UVB irradiated (200 mJ/cm^2). Sunburn cells and TUNEL-positive cells are indicated by arrowheads. The scale bar indicates 25 μm. **(b)** The numbers of TUNEL-positive nuclei of MIF Tg mice were compared with the WT mice. Each value represents the mean ± SEM ($n = 5$). Smaller numbers of TUNEL-positive cells were observed in the MIF Tg in comparison with the WT mouse skin (*$P < 0.01$).

(31) in UVB-irradiated skin. Twenty-four or 48 hours after 200 mJ/cm^2 UVB irradiation, a large number of CPD-positive cells was detected in MIF Tg mice. Whereas, there were fewer CPD-positive cells detected in WT mice (Figure 4a). Thereafter, the number of CPD-positive cell in the MIF Tg mice was significantly higher compared with that in the WT mice ($P < 0.001$; Figure 4b).

p53, bax and p21 expression in UV-irradiated MIF Tg mice epidermis

p53 is a key factor in the photoreactive process and bax and p21 are important downstream proteins regulated by p53. To further confirm the role of MIF in influencing p53-mediated gene activation, the time course for the induction of p53, bax and p21 in 200 mJ/cm^2 UVB-irradiated mouse epidermis was investigated by western blot analysis with specific antibodies. The epidermis derived from MIF Tg mice exhibited decreased induction levels of p53 at 12 and 24 h after irradiation in comparison with the WT mice (Figure 5a). Similarly, the induction levels of bax and p21 from the MIF Tg mice substantially decreased in comparison with those of the WT mice at 48 and 72 h after UVB exposure. An immunohistochemical analysis revealed that at 24 h after UVB irradiation, intense nuclear p53 immunostaining was observed in the WT mice epidermis. In contrast, nuclear p53 immunostaining was low in the MIF Tg mice (Figure 5b). Similarly, at 48 h after UVB irradiation, a low level of p21 expression in and around the nuclei was observed in the MIF Tg mice in comparison with the WT mice. Bax immunoreactivity was both perinuclear and cytoplasmic and the MIF Tg mice showed a lower expression level compared with that of the WT mice at 48 h (Figure 5b).

UVB-induced cutaneous inflammation in MIF Tg and WT mice

UVB-induced infiltration of leukocytes is a major source of inflammatory reactions. Therefore, the effect of UVB-induced infiltration was examined in MIF Tg and WT mice after three courses of UVB exposure. UVB exposure in the MIF Tg mice resulted in greater leukocyte infiltration than in the UVB-irradiated WT mice skin ($P < 0.05$; Figure 6).

UVB-induced apoptosis in cultured keratinocytes of MF Tg and WT mice

To confirm that MIF overexpression prevents keratinocyte apoptosis, cultured keratinocyte from the MIF Tg or the WT mice were irradiated with UVB at 50 mJ/cm^2. After 24 h, irradiated cells were analyzed for TUNEL assay or western blot for p53. As shown in Figure 7a and b, apoptotic keratinocytes (TUNEL positive) from MIF Tg mice were significantly reduced compared with that of WT mice ($P < 0.005$). Furthermore p53 expression of MIF Tg keratinocytes was also lower than that of WT mice (Figure 7c).

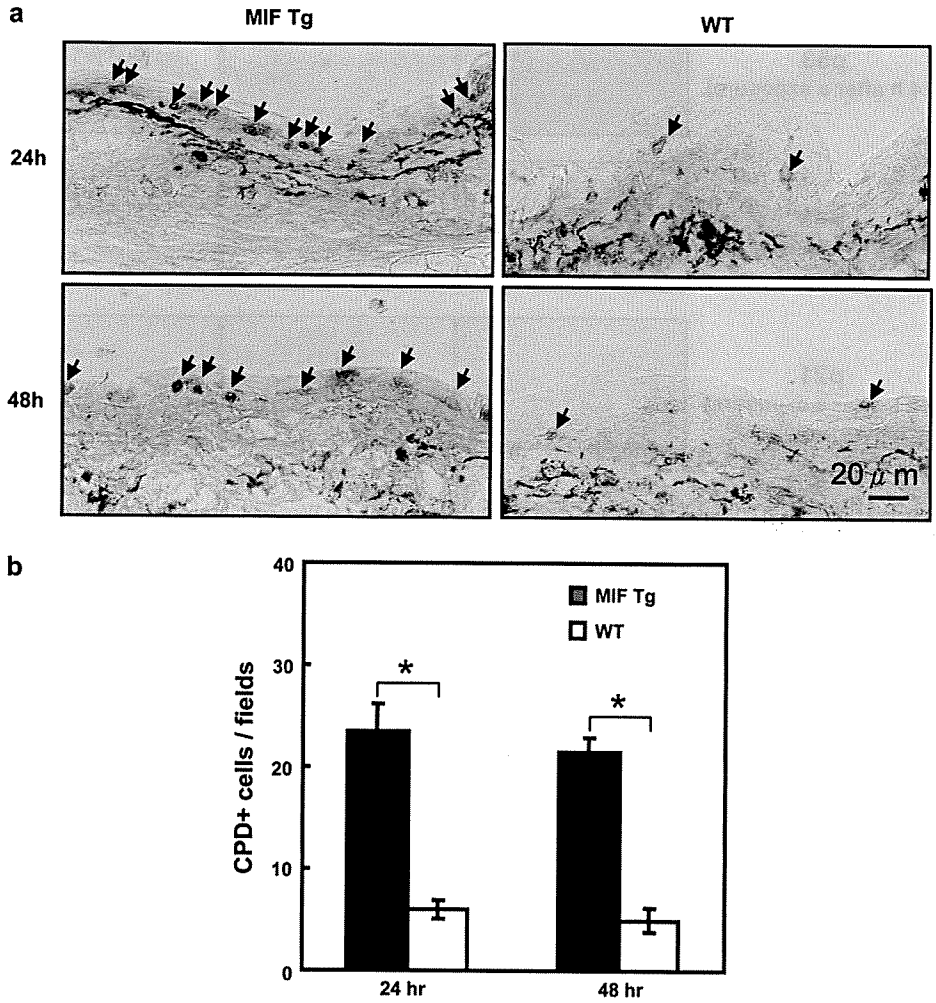

Fig. 4. CPD-positive cells in UV-irradiated MIF Tg mouse epidermis. (**a**) CPD staining in the epidermis of MIF Tg and WT mice skin 24 or 48 h after UVB irradiated (200 mJ/cm^2). CPD-positive cells indicated by arrowheads. Scale bar indicates 20 μm. (**b**) The numbers of CPD-positive cells of MIF Tg mice were compared with WT mice. Each value represents the mean ± SEM ($n = 5$) (*$P < 0.001$).

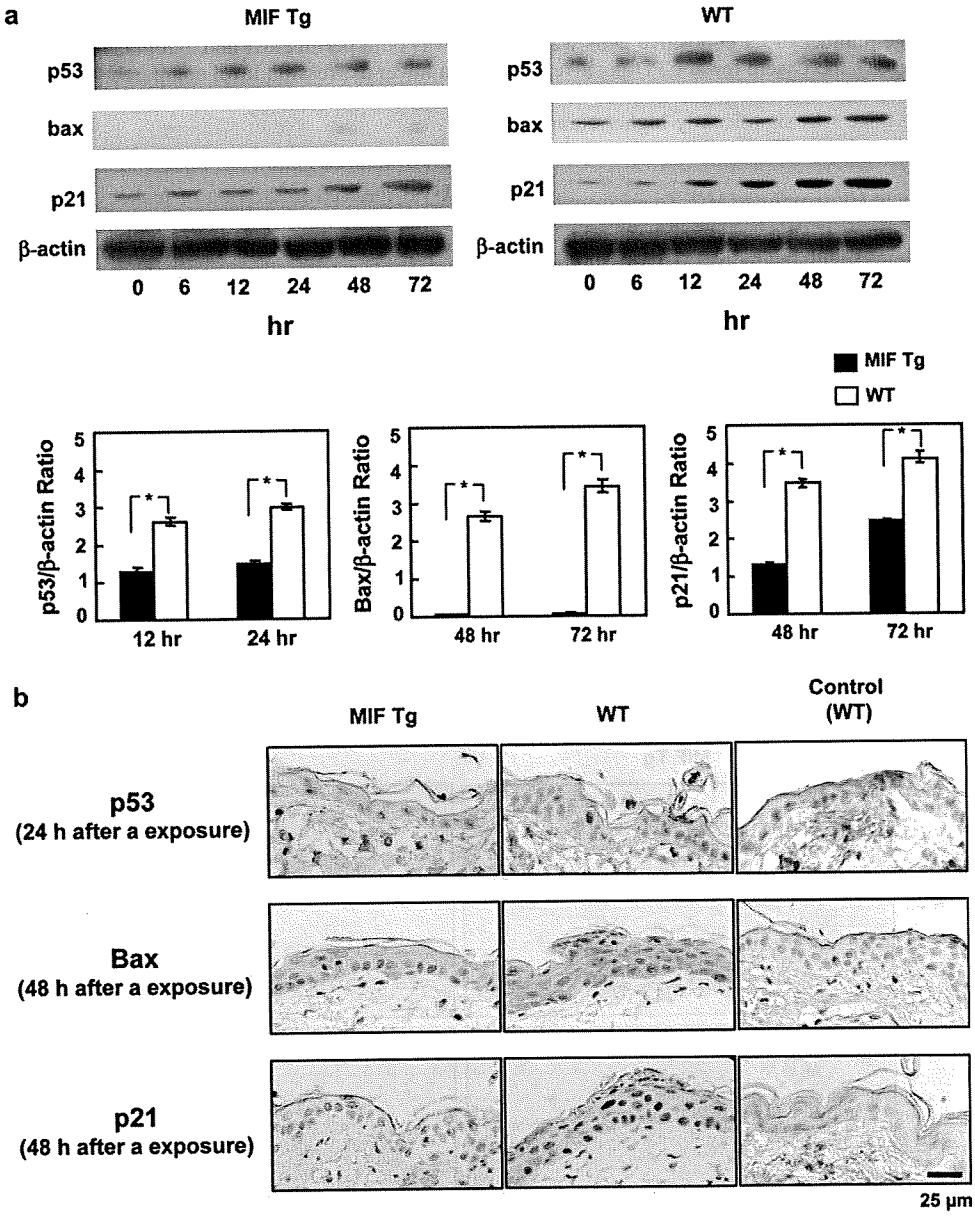

Fig. 5. p53, bax and p21 protein expression in UV-irradiated MIF Tg and WT mice epidermis. (**a**) Western blot analysis of p53, bax and p21 protein expression in unirradiated (0 h) and UVB-irradiated MIF Tg and WT mice skin at various time points. The relative amounts of protein associated with specific antibodies were normalized by the intensities of β-actin ($^{*}P < 0.0001$, $^{**}P < 0.001$, $n = 3$). The data shown are representative of three independent experiments. (**b**) Immunohistochemical analysis for p53, bax and p21 proteins in UVB-irradiated MIF Tg and WT mice skin at 24 h of p53 and at 48 h of bax and p21 immunoreactivity. This experiment was repeated three times with similar results. The scale bar indicates 25 μm.

Discussion

Chronic exposure to solar UV irradiation leads to photoaging, immunosuppression and ultimately carcinogenesis in the skin. Apoptosis and enhanced DNA repair are important p53-mediated responses (32). UVB-induced DNA lesions contribute to cell cycle arrest, DNA repair and finally apoptosis when DNA damage is beyond repair. p53/p21 are responsible for these adaptive protective responses. Moreover, p53 also directly participates in the initiation and regulation of the DNA repair procedure. Therefore, it is extremely important that apoptosis is induced quickly after UV irradiation, without any dysregulation. The current study demonstrated that an earlier onset of carcinogenesis and a higher incidence of tumors were observed in the MIF Tg mice compared with the WT mice after chronic UVB irradiation. In addition, the UVB-induced apoptosis of epidermal keratinocytes was inhibited in the MIF Tg mice. Significantly fewer TUNEL-positive cells were detected in MIF Tg mice in comparison with WT mice. There was a decreased expression of apoptosis-regulatory genes, p53, bax and p21 in MIF Tg mice after UVB irradiation in this study. A previous study has already confirmed that similar protective effects were observed in response to acute UVB light in the MIF Tg mice cornea (33). MIF is upregulated by UVB irradiation in mouse cornea and MIF Tg mice had less apoptotic cells. TUNEL staining in the cornea shows a significantly smaller number of TUNEL-positive nuclei in the MIF Tg mice compared with the WT mice after UV exposure (33).

MIF is a cytokine that not only plays a critical role in several inflammatory conditions but also inhibits p53-dependent apoptotic processes (23,24,34). Hudson *et al.* (23) reported that MIF

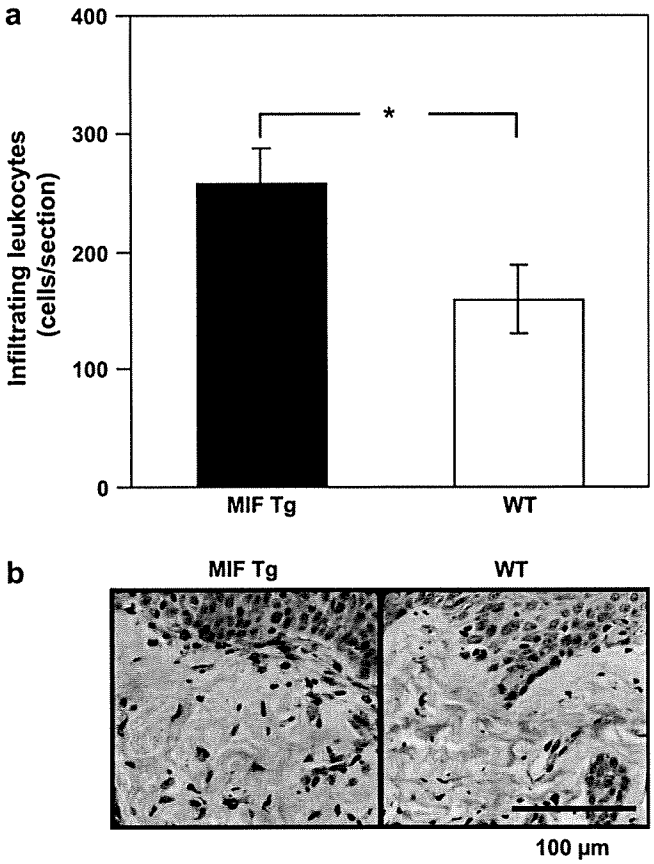

Fig. 6. UVB-induced cutaneous inflammation in MIF Tg and WT mice. (**a**) After three courses of UVB exposure, skin was obtained on day 7 and the paraffin-embedded skin samples (5 μm thick) were processed for routine hematoxylin and eosin staining following a standard protocol. Infiltrating leukocytes (monocyte/macrophages and neutrophils) of the MIF Tg mice were compared with the WT mice. Each value represents the mean ± SEM (n = 5). UVB exposure of MIF Tg mice resulted in greater leukocyte infiltration than that observed in UVB-irradiated WT mice skin (* $P < 0.05$). (**b**) Representative examples of micrographs of hematoxylin and eosin staining are shown from experiments conducted using skin samples (n = 5) that had identical patterns. Bar = 100 μm.

treatment was able to overcome p53 activity and inhibited its transcriptional activity. Recently, Martin *et al.* (35) reported that MIF-deficient mice showed significant increases in p53 activity following acute UVB irradiation, and MIF-deficient mice showed a reduction in tumor incidence in comparison with WT mice following chronic UVB exposure. Previous data from other groups and the current findings suggest that MIF has an inhibitory effect on UVB-induced photodamage by blocking the relevant expression of apoptosis-regulatory genes p53, bax and p21 and MIF plays an important role in UVB-induced tumor development and progression.

The present study also demonstrated that UVB exposure in MIF Tg mice resulted in greater leukocyte infiltration than that of the UVB-irradiated WT mice skin. UVB irradiation enhances the expression of MIF in the epidermis (25) and MIF Tg mice showed higher levels of MIF mRNA expression after UVB exposure in this study. UVB stimulates the production of several proinflammatory cytokines in the skin and these cytokines are known to be involved in the induction of skin carcinogenesis (11,36). For example, TNF-α is the essential cytokine in tumor promotion in mouse skin. Tumor promotion by 12-*O*-tetradecanoylphorbol-13-acetate on the skin of TNF-α-deficient mice decreased in comparison with WT mice. Similarly, tumor promotion in IL-6-deficient mice was significantly decreased by 12-*O*-tetradecanoylphorbol-13-acetate compared with the WT mice (11). UVB-induced inflammatory responses, such as the production of cytokines and the infiltration of inflammatory cells, are clearly linked to the development of skin tumors (3,4). The inhibition of this inflammatory response via topical application of an anti-inflammatory drug inhibits the acute inflammatory responses after UVB exposure and decreases tumor formation after chronic exposure (37). MIF has a direct proinflammatory role in inflammatory conditions and tumorigenesis (38). Once released, MIF acts as a proinflammatory cytokine to induce expression of other inflammatory cytokines, including IL-1, IL-6 and TNF-α. Therefore, intense inflammation in MIF Tg mice in response to UVB irradiation was found to correlate with the early onset of carcinogenesis and the higher incidence of tumors after chronic UVB irradiation.

MIF has a wider spectrum of action and exhibits proneoplastic activity. In many tumor cells and pretumor states, increased MIF mRNA can be detected in prostate (39), colon (40) and hepatocellular cancers (41), adenocarcinomas of the lung (42), glioblastomas (43) and melanomas (9). The role of MIF in proneoplastic activity has been examined by several groups. Fingerle *et al.* reported that embryonic fibroblasts from MIF deficient mice exhibit p53-dependent growth alterations, increased p53 transcriptional activity and resistance to ras-mediated transformation (23,24,34). Concurrent deletion of the p53 gene *in vivo* reversed the observed phenotype of cells deficient in MIF. *In vivo* studies showed that fibrosarcomas are smaller in size and have a lower mitotic index in MIF deficient mice relative to their WT counterparts. They concluded direct genetic evidence for a functional link between MIF and the p53 tumor suppressor (23,24,34). The effectiveness of an anti-MIF antibody on reducing tumor growth and neovascularization in lymphoma cells and vascular endothelial cells *in vivo* has been reported (22). Consistent with this finding, anti-MIF antibodies are effective in reducing tumor angiogenesis in melanoma cells (21). This was demonstrated *in vitro* by recombinant MIF in fibroblasts, where growth factor-induced stimulation of these cells resulted in increased MIF concentrations, activation of the ERK-MAP kinase pathway and a subsequent increase in cell proliferation (44). Meyer-Siegler *et al.* (45) has also shown that the addition of TGFβ results in increased MIF expression in a colon cancer cell line. Furthermore, Abe *et al.* (46) observed an increase in cytotoxic T lymphocytes following MIF inhibition as a result of specific antibodies. Moreover, the number of apoptotic tumor cells increased following MIF inhibition. Tumors arising in the MIF knockdown cells grew less rapidly and also showed an increased degree of apoptosis (47). These findings therefore suggest that once keratinocytes are mutated by UVB-induced DNA damage, they may develop into tumor cell, suggested that MIF has a dual role by promoting tumor cell growth and inhibiting the apoptotic processes.

In conclusion, chronic UVB irradiation induces early onset of skin carcinogenesis and the high incidence of tumors in MIF Tg mice. These findings suggest that chronic UVB exposure enhances MIF production, which may inhibit the p53-dependent apoptotic processes, enhance intensive inflammation and thereby induce photocarcinogenesis in the skin. Consequently, this newly identified mechanism may contribute to our overall understanding of photo-induced skin damage, which results in carcinogenesis. These findings are promising for the potential development of MIF inhibitors for therapeutic use and the treatment of photodamaged skin.

Funding

Ministry of Education, Science and Culture of Japan (No. 20591337).

Acknowledgements

Conflict of Interest Statement: None declared.

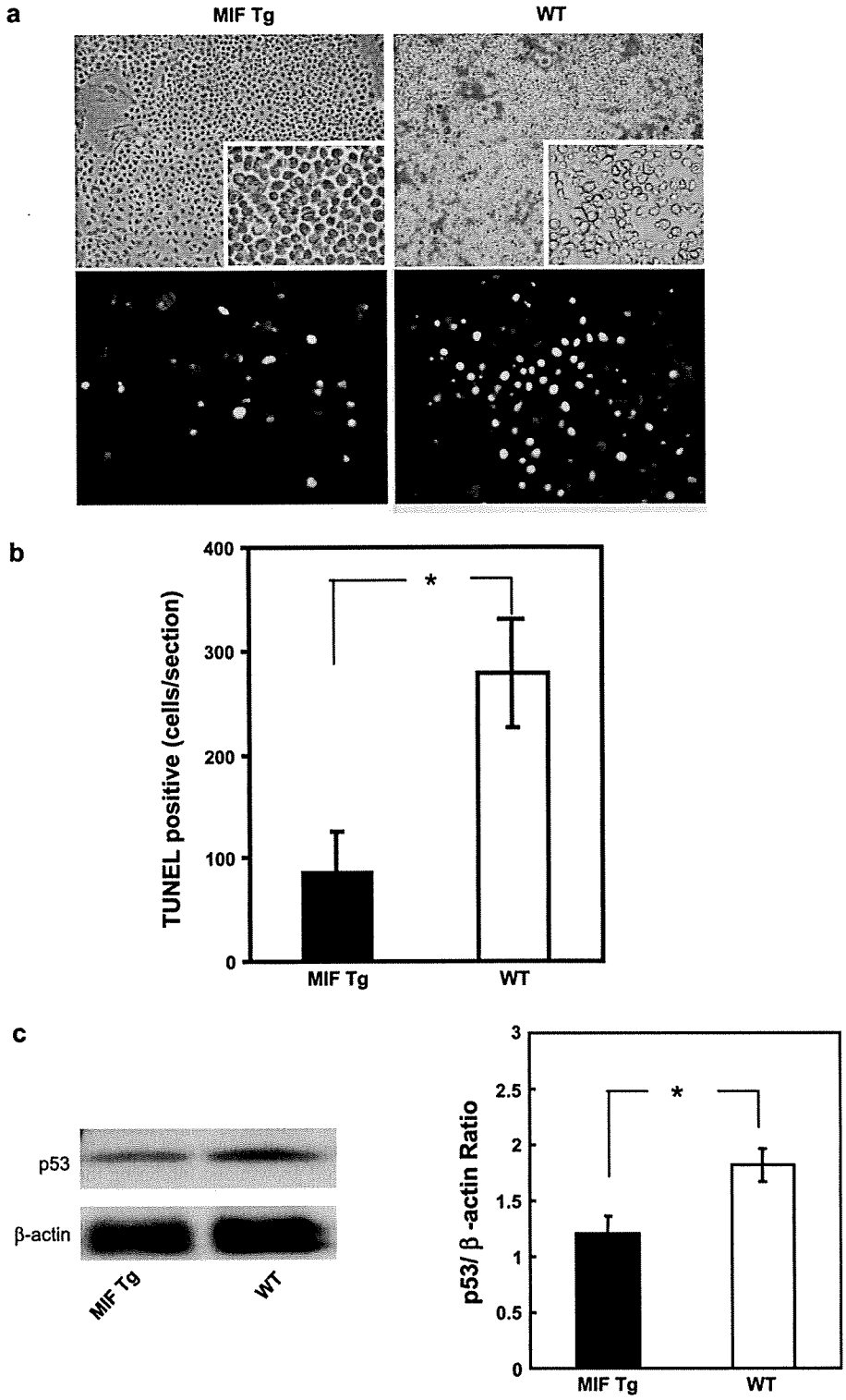

Fig. 7. UVB-induced apoptosis in cultured keratinocytes of MF Tg and WT. (**a**) Cultured keratinocyte from the MIF Tg or WT mice were irradiated with UVB at 50 mJ/cm^2. After 24 h, irradiated cells were analyzed for TUNEL assay. Upper panels indicate morphological pictures. Lower panels indicate TUNEL assay. (**b**) Apoptotic keratinocytes (TUNEL positive) from MIF Tg mice were significantly reduced compared with that of WT mice ($^*P < 0.005$). (**c**) p53 protein expression of UVB-irradiated keratinocytes were analyzed using western blot. The relative amounts of proteins associated with specific antibodies were normalized by the intensities of β-actin. These data shown are representative of three independent experiments. p53 expression of MIF Tg keratinocytes was lower than that of WT mice ($^*P < 0.005$).

References

1. Young,A.R. (1990) Cumulative effects of ultraviolet radiation on the skin: cancer and photoaging. *Semin. Dermatol.*, **9**, 25–31.
2. Kraemer,K.H. (1997) Sunlight and skin cancer: another link revealed. *Proc. Natl Acad. Sci. USA*, **94**, 11–14.
3. Fischer,S.M. *et al.* (1999) Chemopreventive activity of celecoxib, a specific cyclooxygenase-2 inhibitor, and indomethacin against ultraviolet light-induced skin carcinogenesis. *Mol. Carcinog.*, **25**, 231–240.
4. Pentland,A.P. *et al.* (1999) Reduction of UV-induced skin tumors in hairless mice by selective COX-2 inhibition. *Carcinogenesis*, **20**, 1939–1944.
5. Cleaver,J.E. *et al.* (2002) UV damage, DNA repair and skin carcinogenesis. *Front Biosci.*, **7**, d1024–d1043.
6. Stenback,F. *et al.* (1998) p53 expression in skin carcinogenesis and its relationship to cell proliferation and tumour growth. *Eur. J. Cancer*, **34**, 1415–1424.
7. Ansel,J.C. *et al.* (1988) The expression and modulation of IL-1 alpha in murine keratinocytes. *J. Immunol.*, **140**, 2274–2278.
8. Kupper,T.S. *et al.* (1987) Interleukin 1 gene expression in cultured human keratinocytes is augmented by ultraviolet irradiation. *J. Clin. Invest.*, **80**, 430–436.
9. Kirnbauer,R. *et al.* (1991) Regulation of epidermal cell interleukin-6 production by UV light and corticosteroids. *J. Invest. Dermatol.*, **96**, 484–489.
10. Kock,A. *et al.* (1990) Human keratinocytes are a source for tumor necrosis factor alpha: evidence for synthesis and release upon stimulation with endotoxin or ultraviolet light. *J. Exp. Med.*, **172**, 1609–1614.
11. Suganuma,M. *et al.* (2002) Discrete roles of cytokines, TNF-alpha, IL-1, IL-6 in tumor promotion and cell transformation. *Int. J. Oncol.*, **20**, 131–136.
12. Bloom,B.R. *et al.* (1966) Mechanism of a reaction *in vitro* associated with delayed-type hypersensitivity. *Science*, **153**, 80–82.
13. David,J.R. (1966) Delayed hypersensitivity *in vitro*: its mediation by cell-free substances formed by lymphoid cell-antigen interaction. *Proc. Natl Acad. Sci. USA*, **56**, 72–77.
14. Bernhagen,J. *et al.* (1993) MIF is a pituitary-derived cytokine that potentiates lethal endotoxaemia. *Nature*, **365**, 756–759.
15. Calandra,T. *et al.* (1994) The macrophage is an important and previously unrecognized source of macrophage migration inhibitory factor. *J. Exp. Med.*, **179**, 1895–1902.
16. Lanahan,A. *et al.* (1992) Growth factor-induced delayed early response genes. *Mol. Cell Biol.*, **12**, 3919–3929.
17. Wistow,G.J. *et al.* (1993) A macrophage migration inhibitory factor is expressed in the differentiating cells of the eye lens. *Proc. Natl Acad. Sci. USA*, **90**, 1272–1275.
18. Bucala,R. (1996) MIF re-discovered: pituitary hormone and glucocorticoid-induced regulator of cytokine production. *Cytokine Growth Factor Rev.*, **7**, 19–24.
19. Bacher,M. *et al.* (1997) Migration inhibitory factor expression in experimentally induced endotoxemia. *Am. J. Pathol.*, **150**, 235–246.
20. Nishihira,J. (2000) Macrophage migration inhibitory factor (MIF): its essential role in the immune system and cell growth. *J. Interferon Cytokine Res.*, **20**, 751–762.
21. Shimizu,T. *et al.* (1999) High expression of macrophage migration inhibitory factor in human melanoma cells and its role in tumor cell growth and angiogenesis. *Biochem. Biophys. Res. Commun.*, **264**, 751–758.
22. Chesney,J. *et al.* (1999) An essential role for macrophage migration inhibitory factor (MIF) in angiogenesis and the growth of a murine lymphoma. *Mol. Med.*, **5**, 181–191.
23. Hudson,J.D. *et al.* (1999) A proinflammatory cytokine inhibits p53 tumor suppressor activity. *J. Exp. Med.*, **190**, 1375–1382.
24. Nemajerova,A. *et al.* (2007) Impaired DNA damage checkpoint response in MIF-deficient mice. *EMBO J.*, **26**, 987–997.
25. Shimizu,T. *et al.* (1999) Ultraviolet B radiation upregulates the production of macrophage migration inhibitory factor (MIF) in human epidermal keratinocytes. *J. Invest. Dermatol.*, **112**, 210–215.
26. Watanabe,H. *et al.* (2004) Ultraviolet A-induced production of matrix metalloproteinase-1 is mediated by macrophage migration inhibitory factor (MIF) in human dermal fibroblasts. *J. Biol. Chem.*, **279**, 1676–1683.
27. Shimizu,T. *et al.* (1997) Macrophage migration inhibitory factor is an essential immunoregulatory cytokine in atopic dermatitis. *Biochem. Biophys. Res. Commun.*, **240**, 173–178.
28. Sasaki,S. *et al.* (2004) Transgene of MIF induces podocyte injury and progressive mesangial sclerosis in the mouse kidney. *Kidney Int.*, **65**, 469–481.
29. Akagi,Y. *et al.* (1997) Transcriptional activation of a hybrid promoter composed of cytomegalovirus enhancer and beta-actin/beta-globin gene in glomerular epithelial cells *in vivo*. *Kidney Int.*, **51**, 1265–1269.
30. Noonan,F.P. *et al.* (2000) Accelerated ultraviolet radiation-induced carcinogenesis in hepatocyte growth factor/scatter factor transgenic mice. *Cancer Res.*, **60**, 3738–3743.
31. Arad,S. *et al.* (2008) Topical thymidine dinucleotide treatment reduces development of ultraviolet-induced basal cell carcinoma in Ptch-1+/- mice. *Am. J. Pathol.*, **172**, 1248–1255.
32. Levine,A.J. (1997) p53, the cellular gatekeeper for growth and division. *Cell*, **88**, 323–331.
33. Kitaichi,N. *et al.* (2008) Macrophage migration inhibitory factor ameliorates UV-induced photokeratitis in mice. *Exp. Eye Res.*, **86**, 929–935.
34. Fingerle-Rowson,G. *et al.* (2003) The p53-dependent effects of macrophage migration inhibitory factor revealed by gene targeting. *Proc. Natl Acad. Sci. USA*, **100**, 9354–9359.
35. Martin,J. *et al.* (2008) Macrophage migration inhibitory factor (MIF) plays a critical role in pathogenesis of ultraviolet-B (UVB) -induced nonmelanoma skin cancer (NMSC). *FASEB J.*, **23**, 720–730.
36. Moore,R.J. *et al.* (1999) Mice deficient in tumor necrosis factor-alpha are resistant to skin carcinogenesis. *Nat. Med.*, **5**, 828–831.
37. Wilgus,T.A. *et al.* (2003) Inhibition of cutaneous ultraviolet light B-mediated inflammation and tumor formation with topical celecoxib treatment. *Mol. Carcinog.*, **38**, 49–58.
38. Bach,J.P. *et al.* (2008) Role of MIF in inflammation and tumorigenesis. *Oncology*, **75**, 127–133.
39. Meyer-Siegler,K. *et al.* (1998) Expression of macrophage migration inhibitory factor in the human prostate. *Diagn. Mol. Pathol.*, **7**, 44–50.
40. Legendre,H. *et al.* (2003) Prognostic values of galectin-3 and the macrophage migration inhibitory factor (MIF) in human colorectal cancers. *Mod. Pathol.*, **16**, 491–504.
41. Ren,Y. *et al.* (2003) Macrophage migration inhibitory factor: roles in regulating tumor cell migration and expression of angiogenic factors in hepatocellular carcinoma. *Int. J. Cancer*, **107**, 22–29.
42. Kamimura,A. *et al.* (2000) Intracellular distribution of macrophage migration inhibitory factor predicts the prognosis of patients with adenocarcinoma of the lung. *Cancer*, **89**, 334–341.
43. Rogge,L. (2002) A genomic view of helper T cell subsets. *Ann. N. Y. Acad. Sci.*, **975**, 57–67.
44. Takahashi,N. *et al.* (1998) Involvement of macrophage migration inhibitory factor (MIF) in the mechanism of tumor cell growth. *Mol. Med.*, **4**, 707–714.
45. Meyer-Siegler,K.L. *et al.* (2006) Inhibition of macrophage migration inhibitory factor or its receptor (CD74) attenuates growth and invasion of DU-145 prostate cancer cells. *J. Immunol.*, **177**, 8730–8739.
46. Abe,R. *et al.* (2001) Regulation of the CTL response by macrophage migration inhibitory factor. *J. Immunol.*, **166**, 747–753.
47. Hagemann,T. *et al.* (2007) Ovarian cancer cell-derived migration inhibitory factor enhances tumor growth, progression, and angiogenesis. *Mol. Cancer Ther.*, **6**, 1993–2002.

Received March 2, 2009; revised June 15, 2009; accepted June 20, 2009

Immunological Reconstitution after Autologous Hematopoietic Stem Cell Transplantation in Patients with Systemic Sclerosis: Relationship Between Clinical Benefits and Intensity of Immunosuppression

TOSHIYUKI BOHGAKI, TATSUYA ATSUMI, MIYUKI BOHGAKI, AKIRA FURUSAKI, MAKOTO KONDO, KAZUKO C. SATO-MATSUMURA, RIICHIRO ABE, HIROSHI KATAOKA, TETSUYA HORITA, SHINSUKE YASUDA, YOSHIHARU AMASAKI, MITSUFUMI NISHIO, KEN-ICHI SAWADA, HIROSHI SHIMIZU, and TAKAO KOIKE

ABSTRACT. ***Objective.*** To analyze the relationship between clinical benefits and immunological changes in patients with systemic sclerosis (SSc) treated with autologous hematopoietic stem cell transplantation (HSCT).

Methods. Ten patients with SSc were treated with high-dose cyclophosphamide followed by highly purified CD34+ cells (n = 5) or unpurified grafts (n = 5). Two groups of patients were retrospectively constituted based on their clinical response (good responders, n = 7; and poor responders, n = 3). As well as clinical findings, immunological reconstitution through autologous HSCT was assessed by fluorescence-activated cell sorter analysis, quantification of signal joint T cell receptor rearrangement excision circles (sjTREC), reflecting the thymic function, and *foxp3*, a key gene of regulatory T cells, mRNA levels.

Results. Patients' clinical and immunological findings were similar between good and poor responders, or CD34-purified and unpurified groups at inclusion. The sjTREC values were significantly suppressed at 3 months after autologous HSCT in good responders compared with poor responders (p = 0.0152). Reconstitution of CD4+CD45RO- naive T cells was delayed in good responders compared with poor responders. The phenotype of other lymphocytes, cytokine production in T cells, and *foxp3* gene expression levels after autologous HSCT did not correlate with clinical response in good or poor responders. Clinical and immunological findings after autologous HSCT were similar between CD34-purified and unpurified groups.

Conclusion. Our results suggest that immunosuppression intensity, sufficient to induce transient suppression of thymic function, is attributable to the feasible clinical response in patients with SSc treated with autologous HSCT. Appropriate monitoring of sjTREC values may predict clinical benefits in transplanted SSc patients after autologous HSCT. (First Release May 15 2009; J Rheumatol 2009;36:1240–8; doi:10.3899/jrheum.081025)

Key Indexing Terms:
SYSTEMIC SCLEROSIS HEMATOPOIETIC STEM CELL TRANSPLANTATION
IMMUNOLOGICAL RECONSTITUTION

From the Department of Medicine II and the Department of Dermatology, Hokkaido University Graduate School of Medicine, Sapporo; and Third Department of Internal Medicine, Akita University School of Medicine, Akita, Japan.

Supported by a grant from the Japanese Ministry of Health, Labor and Welfare.

T. Bohgaki, MD, PhD; T. Atsumi, MD, PhD; M. Bohgaki, MD, PhD; A. Furusaki, MD, PhD; M. Kondo, MD, PhD, Department of Medicine II; K.C. Sato-Matsumura, MD, PhD; R. Abe, MD, PhD, Department of Dermatology; H. Kataoka, MD, PhD; T. Horita, MD, PhD; S. Yasuda, MD, PhD; Y. Amasaki, MD, PhD; M. Nishio, MD, PhD, Department of Medicine II, Hokkaido University Graduate School of Medicine; K. Sawada, MD, PhD, Third Department of Internal Medicine, Akita University School of Medicine; H. Shimizu, MD, PhD, Department of Dermatology; T. Koike, MD, PhD, Department of Medicine II, Hokkaido University School of Medicine.

Address reprint requests to Dr. T. Atsumi, Department of Medicine II, Hokkaido University Graduate School of Medicine, N15, W7, Kita-ku, Sapporo 060-8638, Japan. E-mail: at3tat@med.hokudai.ac.jp

Accepted for publication January 8, 2009.

Systemic sclerosis (SSc) is an autoimmune disease characterized by the presence of skin sclerosis, organ fibrosis, and autoantibodies[1]. Despite extensive research on autoimmunology and endotheliology, its pathophysiology has been far from conclusive[2,3]. The skin and organ manifestations of SSc are, in general, slowly progressive and chronically disabling. In some patients, however, they can be rapidly progressive and fatal due to organ involvements such as interstitial pneumonia, arrhythmia, and renal failure. Severe organ involvement frequently occurs within the first 3 years of disease[1]. These clinical features affect daily living activity and life expectancy in patients with SSc.

Autologous hematopoietic stem cell transplantation (HSCT) has been indicated for patients with autoimmune diseases, resulting in great success particularly in patients with SSc[4-10]. Autologous HSCT is one of the treatments in

patients suffering from hematological malignant diseases. For the practice of autologous HSCT against those malignant diseases, graft manipulation using antibody specific for CD34, a marker of human hematopoietic stem cells, is usually essential to deplete malignant cells from the graft. On the other hand, patients treated with CD34+-selected autologous HSCT (CD34-HSCT) may have infectious complications during hematological recovery more frequently than patients treated with unselected autologous HSCT (unselected-HSCT)[11]. The graft manipulation was performed in many patients with severe autoimmune diseases treated by autologous HSCT in consideration of depleting autoreactive lymphocytes and inducing profound clinical remission. Meanwhile, it has been debated whether CD34+ cell selection in the graft is necessary or not[9,12].

The difference in conditioning regimens is not related to the clinical benefits, and about one-third of transplanted patients do not benefit from these intensive immunosuppressive treatment[9,13]. Clinical response may depend on profound qualitative immunological changes obtained by autologous HSCT in patients with systemic lupus erythematosus or multiple sclerosis[14,15]. Little is known as to why and how patients with SSc have clinical benefits of autologous HSCT. The aim of our study was to elucidate the relationship between clinical effect and alteration of immunological profiles in patients with SSc treated with autologous HSCT.

MATERIALS AND METHODS

Patients. Our study was approved by the ethical committee of Hokkaido University and written informed consent was obtained from all participants. Thirty-one patients with SSc, all of whom met the American College of Rheumatology preliminary criteria[16], were screened for our study. All patients developing SSc within the last 3 years onset fulfilled at least 1 of the following: early rapidly progressive diffuse skin sclerosis despite continuing treatment, refractory skin ulcers, interstitial lung disease confirmed by lung computed tomography (CT), reversible cardiac involvement such as arrhythmia and cardiomegaly, renal involvement with hypertension, persistent urinalysis abnormalities, and microangiopathic hemolytic anemia. Patients were excluded from the study when they were over 60 years old, or had uncontrolled arrhythmia, left ventricular ejection fraction on echocardiography below 45%, carbon dioxide diffusion lung capacity (DLCO) below 45% predicted, serum creatinine above 176.8 μmol/L (2.0 mg/dl) and glomerular filtration rate (GFR) below 40 ml/min/m^2. All enrolled patients were evaluated clinically at the time of diagnosis and on regular visits for followup.

Thirty-five healthy controls were also enrolled in the study.

Transplantation procedure and followup. The mobilization regimen comprised recombinant human granulocyte colony-stimulating factor (rhG-CSF) and intravenous cyclophosphamide (4 g/m^2). In 5 patients treated with CD34-HSCT, enriched CD34+ graft, prepared using CliniMACS® system (Miltenyi Biotec, Germany) was stored in liquid nitrate until use for transplant. Graft manipulation was not performed in the next 5 patients treated with unselected-HSCT.

We treated all SSc patients with intravenous cyclophosphamide (200 mg/kg, divided into 4 days) followed by autologous HSCT. rhG-CSF was administered from the second day of transplantation of frozen-thawed autologous enriched CD34+ grafts or frozen-thawed autologous unselected grafts. T cell depleting antibodies such as antithymocyte globulin, antilymphocyte globulin and anti-CD52 antibodies (Campath) were not administered in our patients.

We assessed the improvement of skin sclerosis by the modified Rodnan total thickness skin score (mRTSS). Electrocardiogram and echocardiography were used to evaluate the cardiac function, chest radiograph, chest high resolution CT, and spirometry to evaluate pulmonary function, renogram to evaluate renal function, and serological tests to assess other organ involvement and the presence of autoantibodies.

Lymphocyte phenotyping. Peripheral blood mononuclear cells (PBMC) were prepared from heparinized venous blood by Ficoll-Paque Plus® (Amersham Biosciences Corp., NJ, USA).

We assessed the subpopulation of peripheral lymphocytes by immunofluorescence staining of PBMC with anti-human CD3-Cy-Chrome, CD4-fluorescein isothiocyanate (FITC), CD8-FITC, CD19-FITC, TCRγδ-FITC, CD3-phycoerythrin (PE), CD8-PE, CD45RO-PE, CD25-PE, HLA-DR-PE, and CD69-PE (BD Biosciences Pharmingen, San Diego, CA).

The expression levels of interferon (IFN)-γ and interleukin (IL)-4 were studied in the cytoplasm of peripheral CD4+ or CD8+ T cells. Briefly, we stimulated PBMC with phorbol myristate acetate (50 ng/ml) and ionomycin (250 ng/ml) for 6 h in RPMI 1640 containing 10% heat-inactivated fetal bovine serum and monensin (2 μM) at 37°C in 5% carbon dioxide. We evaluated the IFN-γ or IL-4 expression on T cells by staining with anti-CD3-Cy-Chrome, anti-CD8-FITC and -PE, anti-IFN-γ-FITC, and anti-IL-4-PE using Cytofix/Cytoperm Plus® (BD Biosciences Pharmingen) according to the manufacturer's instructions. Immunostained cells were analyzed using a FACSCalibur™ flow cytometer (Becton Dickinson Immunocytometry Systems, San Jose, CA).

Quantification of thymic signal joint T cell receptor rearrangement excision circles (sjTREC). Thymic sjTREC on genomic DNA from PBMC was quantified by real-time quantitative polymerase chain reaction (PCR) (ABI PRISM® 7000; Applied Biosystems, Foster City, CA) according to the method of Douek, *et al*[17]. The sjTREC values were corrected by the percentage of CD3+ cells in the sample and were then expressed as numbers of sjTREC/μg of CD3+ cells DNA according to the method of Farge, *et al*[18]. Values were measured before autologous HSCT, then at 3, 6, and 12 months after autologous HSCT.

Quantification of foxp3 *gene expression levels.* Total RNA were isolated from PBMC using TRIzol® reagent (Invitrogen, Carlsbad, CA) according to the manufacturer's instructions. Total RNA (1 μg) was reverse transcribed by ReverTraAce (Toyobo, Osaka, Japan), in the presence of oligo(dT)12-18 primers (Invitrogen) according to the manufacturer's instructions. We performed real-time PCR using the ABI PRISM® 7000 Sequence Detection System and specific primers for *foxp3* and *gapdh* from TaqMan® Gene Expression Assays (Applied Biosystems).

Statistical analysis. We used the Mann-Whitney U-test to analyze the difference among each value otherwise indicated. The changes in mRTSS and phenotype of lymphocytes after the autologous HSCT were compared with values at inclusion using the Wilcoxon signed rank test. Female-male ratio in each group was assessed using Fisher's exact probability test. The sjTREC values in healthy individuals were assessed using the Spearman's correlation test. Calculations were performed using the statistical software package JMP version 5.0 (SAS Institute Inc., Cary, NC). P values less than 0.05 were considered significant.

RESULTS

Between November 2000 and July 2006, 11 consecutive patients meeting the criteria in our study were enrolled and 10 patients were transplanted out of 31 screened patients with SSc for autologous HSCT treatment. One patient was not transplanted because of her mobilization failure. First 5 patients were treated with CD34-HSCT. Subsequent 5 patients were treated with unselected-HSCT. The character-

istics of patients treated with autologous HSCT are shown in Table 1. Mean age at inclusion, mean mRTSS before mobilization and mean durations from SSc onset to the treatment were similar between patients treated with CD34-HSCT and unselected-HSCT. Several treatments such as D-penicillamine, prostaglandin derivatives, and corticosteroids were not feasible for our patients. All patients were followed up until July 2007 (40.7 ± 25.6 mos).

Mean number of infused CD34+ cells was not different between CD34-HSCT and unselected-HSCT groups. Mean time needed to achieve a neutrophil count greater than 0.5 × 10^9/l and a platelet count greater than 50 × 10^9/l were not different between 2 groups. Cytomegalovirus antigenemia were shown in 3 patients out of all transplanted patients. Patient 2 had hemophagocytic syndrome on day 6. Patient 3 had adenoviral hemorrhagic cystitis on day 14 and engraftment syndrome on day 15. Patient 7 had engraftment syndrome on day 12. Hemophagocytic syndrome and engraftment syndrome responded to corticosteroid administration. Hemorrhagic cystitis was refractory to acyclovir, vidarabine, ganciclovir, or ribavirin. Patient 3 had the second autologous HSCT using unselected grafts at 3 months after first autologous HSCT using selected CD34+ cells due to recurrent infectious diseases.

Four out of 5 transplanted patients have more than a 25% fall in the skin score compared with baseline values in both groups (Figure 1). Dermal thickness assessed by skin biopsy was also improved in these patients with clinical benefits (data not shown). Additional unselected-HSCT at 3 months after CD34-HSCT did not affect Patient 3's skin manifestation. Cardiac and pulmonary functions were not altered significantly through the treatment in all patients (data not shown). Their serum level of γ-globulin almost remained normal range through autologous HSCT (data not shown). Their serum level of anti-Scl70 antibodies reduced except Patient 2 treated with CD34-HSCT (data not shown). Transplantation related complications during hospitalization are shown in Table 1. There was no significant difference in the incidence of adverse events between both groups and no transplantation related mortality.

We compared immunological reconstitution profile over time between good and poor response groups, and between CD34-HSCT and unselected-HSCT groups. First, we analyzed immunological reconstitution between good and poor response groups. Clinical response to therapy was categorized into major, partial, or no response, or disease progression or relapse according to the method of Farge, *et al*[13]. According to the observed clinical response compared to these criteria, 2 groups of patients were retrospectively constituted: good response group, consisting of 7 patients with sustained major or partial response, and poor response group, consisting of 3 patients (Patient 5, 6, and 7) with no

Table 1. Patients' profile at study inclusion and clinical findings at autologous hematopoietic stem cell transplantation (HSCT).

	Patients Treated with CD34-HSCT					Patients treated with Unselected-HSCT					Mean ± SD		
	1	2	3	4	5	6	7	8	9	10	CD34	Untreated	p
Age, yrs	57	19	54	48	52	43	19	42	30	28	46.0 ± 15.4	32.4 ± 10.1	0.094
Sex, female:male	M	F	F	F	M	M	F	F	F	F	3:2	4:1	1.000
mRTSS, 0–51	38	28	25	15	32	32	17	26	23	20	27.6 ± 8.6	23.6 ± 5.8	0.402
Disease duration, mo	21	31	21	12	36	16	24	18	8	12	24.2 ± 9.4	15.6 ± 6.1	0.141
Interstitial pneumonia	—	—	+	—	+	—	+	—	—	—	—	—	—
GFR, ml/min	76.53	121.43	101.43	114.39	99.32	139.29	120.3	101.8	82.62	103.42	102.6 ± 17.2	109.5 ± 21.3	0.465
DLCO %	83	66.8	52.2	90.9	83.8	92.5	54.7	113.4	48	94.4	75.3 ± 15.7	80.6 ± 28.0	0.465
γ-globulin, %	19.5	24.7	24.1	16.8	12.5	20.5	19.8	—	16.8	16.7	19.5 ± 5.1	18.5 ± 2.0	0.712
Anti-Scl 70, index	< 5	92.3	204.6	8.7	158.6	16.1	128.2	< 5	< 5	202	92.8 ± 90.2	69.3 ± 91.5	0.597
Prior therapies	PG	PG, D, PSL	PG, PSL	PG, PSL	D, PSL	PG	PG	D, PSL	D, PSL	PG	—	—	—
Mobilization	G	G + CYC	G + CYC	G + CYC	G + CYC	G + CYC	G + CYC	G + CYC	G + CYC	G + CYC	—	—	—
Conditioning	CYC	CYC	CYC	CYC	CYC	CYC	CYC	CYC	CYC	CYC	—	—	—
Infused CD34+ cells, × 10^6/kg	2.96	5.21	2.75	3.14	12.7	3.95	2.77	4.28	14.9	2.81	5.4 ± 4.2	5.7 ± 5.2	0.917
Purity, %	96	95	90	93.53	96.59	—	—	—	—	—	94.2 ± 2.6	—	—
Neutrophils > 0.5 × 10^9/l (day)	11	9	11	9	9	8	11	10	10	10	9.8 ± 1.1	9.8 ± 1.1	0.914
Platelets > 50 × 10^9/l (day)	15	21	16	8	11	0	8	11	11	12	14.2 ± 5.0	8.4 ± 4.9	0.138
Transplant related complications	CMV	CMV, HPS	CMV, HC, ES	—	—	—	ES	—	—	—	—	—	—

mRTSS: modified Rodnan total thickness skin score; PG: prostaglandin derivatives; D: d-penicillamine; PSL: prednisolone; G: granulocyte-colony-stimulating factor; CYC: cyclophosphamide; CMV: cytomegalovirus antigenemia; HPS: hemophagocytic syndrome; HC: hemorrhagic cystitis; ES: engraftment syndrome; GFR: glomerular filtration rate; DLCO: diffusion capacity for carbon monoxide.

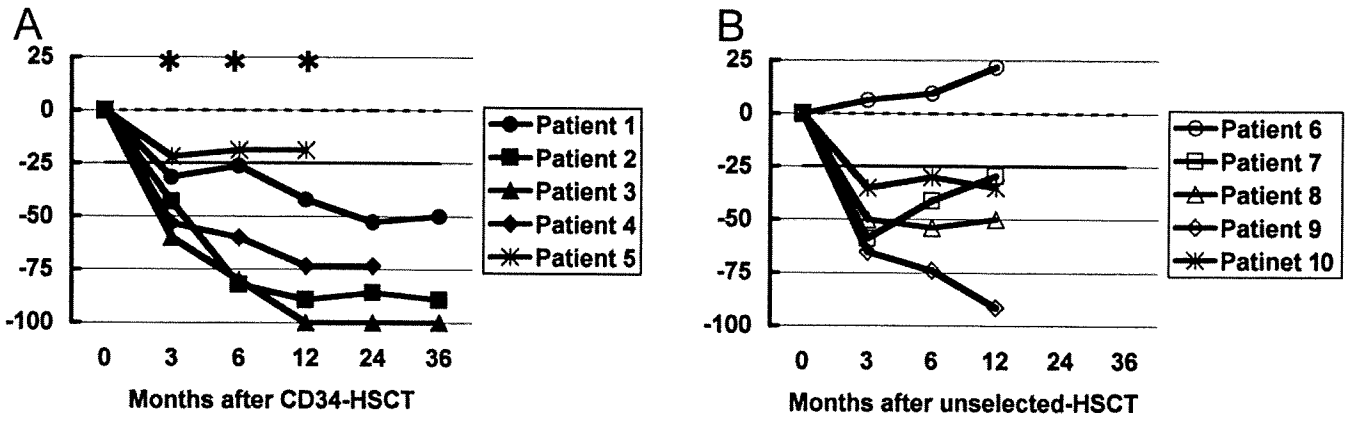

Figure 1. Evaluation of modified Rodnan total thickness skin score (mRTSS) in patients with systemic sclerosis. A. Changes of mRTSS in patients treated with CD34-HSCT. B. Changes of mRTSS in patients treated with unselected-HSCT. Proportional change from baseline measurement was calculated for each patient at each available timepoint. * $p < 0.05$.

response or with relapse of disease (Table 2). Our patients were evaluated by functional evaluation (performance status and/or health assessment questionnaire) and mRTSS with skin improvement assessed by skin biopsy. Each organ function was not altered significantly through the treatment in all patients. Mean age at inclusion, mean mRTSS before mobilization, and mean durations from onset scleroderma to treatment were similar between both groups. At inclusion, the ratio of CD4/CD8, the percentage of CD4+CD45RO+, CD4+CD45RO-, CD19+, CD4+CD25+, CD56+, CD3+TCRγδ+, IFN-γ- and IL-4-producing CD4+ and CD8+ cells were in the normal range for all patients and were not different between good and poor response groups (Table 3). After autologous HSCT, shortened CD4/CD8 ratio was sustained due to delayed CD4+ cell recovery and prompt CD8+ cell recovery in both groups. CD4+CD45RO-naive T cells remained low at 6 months after autologous HSCT in good response group, and CD4+CD45RO- cells reconstituted faster in poor response group ($p < 0.05$). CD19+ and CD56+ cells returned into the normal range at 3 months in both groups. The kinetics of other cells through autologous HSCT was not statistically different between good and poor response group in the study. To evaluate the T cell response against mitogen stimulation after autologous HSCT, mean fluorescence intensity of CD69 on CD3+ cells was investigated. CD69 expression levels on CD3+CD8+ and CD3+CD8- cells against mitogen were not different between healthy controls and patients with SSc before autologous HSCT, and its kinetics through autologous HSCT were similar in both groups (Table 3). Cytokine production in CD3+CD8- and CD3+CD8+ T cells was assessed by intracellular staining of IFN-γ and IL-4. Levels of cytokine production in CD3+CD8- and CD3+CD8+ cells were not different between both groups. IFN-γ producing CD8+ T cells increased after autologous HSCT in both groups (Table 3).

Thymic output assessed by sjTREC was analyzed to evaluate the mechanism of peripheral CD4+CD45RO- and CD4+CD25+ proliferation. In healthy controls, the sjTREC values negatively correlated with their age (Figure 2A, $p < 0.0001$, $r^2 = 0.44$). Nine out of 10 transplanted patients could be analyzed in the study. Their sjTREC values also negatively correlated with their age at inclusion of autologous HSCT (Figure 2B, $p = 0.002$, $r^2 = 0.80$). The sjTREC values were not significantly different between patients with SSc before autologous HSCT and age- and sex-matched

Table 2. Patients' profile between good and poor response groups at autologous HSCT.

	Good Response Group (n = 7)	Poor Response Group (n = 3)	p
Graft condition (CD34-HSCT: unselected)	4:3	1:2	1.000
Age, yrs	39.7 ± 14.4	38.0 + 17.1	0.819
Sex female: male	6:1	1:2	1.000
mRTSS (0–51)	25.0 ± 7.16	27.0 ± 8.66	0.568
Disease duration, mo	17.6 ± 7.72	25.3 ± 10.1	0.207
Infused CD34+ cells (× 10^6/kg)	5.15 ± 4.39	6.47 ± 5.42	0.909
Neutrophils > 0.5 × 10^9/l (day)	10.0 ± 0.82	9.33 ± 1.53	0.407
Platelets > 50 × 10^9/l (day)	13.4 ± 4.28	6.33 ± 5.69	0.064

mRTSS: modified Rodnan total thickness skin score.